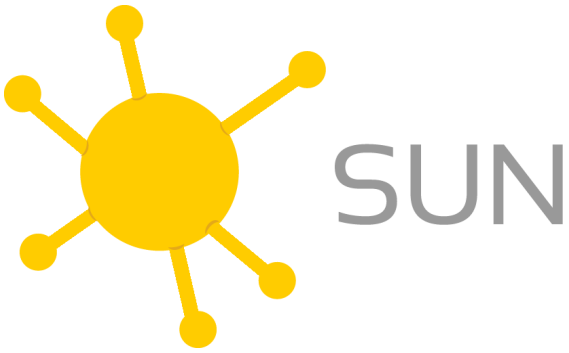

Deliverable report for

SUN

Sustainable Nanotechnologies

Grant Agreement Number 604305

Deliverable D 1.5
Report on characterisation of NOAA in biological samples from (eco)toxicity tests

Due date of deliverable: 30/09/2016

Actual submission date: 02/12/2016

Lead beneficiary for this deliverable: UNIVE - *University Ca' Foscari of Venice*

Dissemination Level:		
PU	Public	
PP	Restricted to other programme participants (including the Commission Services)	
RE	Restricted to a group specified by the consortium (including the Commission Services)	
CO	Confidential, only for members of the consortium (including the Commission Services)	X

Table of Content

Description of Task

The SUstainable Nanotechnology (SUN) project aims at evaluating the environmental and health risks of engineered nanomaterials (ENM) through their life cycle and to use these results for their sustainable manufacturing.
Within the SUN project, WP1 “Case study supply chains and data repository” aims at: I) identifying and acquiring the available data on the SUN case studies; II) constructing and maintaining the SUN database; III) collecting all data (from other projects and literature) relevant for the validation of the tools developed in SUN; IV) acquiring and distributing pristine ENM for (eco)toxicological testing and release experiments; V) characterizing the pristine ENM from (eco)toxicological testing and fate modelling based on available protocols; VI) characterizing ENM in biological samples from (eco)toxicity tests.
According to these objectives, task 1.5 (UNIVE (leader) and VenetoNanotech (VN)) “Characterize NOAA in biological samples from (eco)toxicological tests” has been perfomed with the support of different partners and relevant data has been collected and included in this deliverable.

Description of Work and main achievements

The research activitites can be divided in the three different macroareas as follow:

1. Colloidal characterization of pristine and modified CuO NPs in media relevant for (eco)toxicological testing (partners involved: CNR-ISTEC and UNIVE)
2. Quantification of Cu in tissues and organs from *in vivo* studies (partners involved: RIVM, VN and UNIVE)
3. Other characterization data for SUN samples in other media relevant for (eco)toxicological testing (partner involved: INIA and UoP)

1 CuO nanoparticles colloidal characterization in biological and environmental media

Within a Safety by Design approach, dispersion stability of pristine CuO NPs was improved by using four different non-hazardous stabilizers, leading to positive (polyethylenimine), negative (sodium ascorbate and sodium citrate) and neutral (polyvinylpyrrolidone) surface charge. The synthesis of modified CuO NPs has been already described in D7.1 “Report on the development of SbyD strategies applied to CuO” by CNR-ISTEC. The effects of the different stabilizers on CuO NPs' key determinant properties were investigated in different biological and environmental media by combining Dynamic and Electrophoretic Light Scattering (DLS and ELS), Centrifugal Separation Analysis (CSA) and Inductively coupled plasma optical emission spectroscopy (ICP-OES).

Materials and methods

The colloidal characterization of pristine and modified CuO NPs stock suspensions was performed in: (i) MilliQ water; (ii) Phosphate Buffer Saline (PBS); (iii) Minimum Essential Medium (MEM) and Dulbecco’s Modified Eagle Medium (DMEM), adding 10% v/v Fetal

Bovine Serum (FBS) and 1% v/v Penicillin/Streptomycin (Pen-Strep) according to the concentration used in toxicological tests; (iv) artificial fresh water (AFW) [OECD (1992] and artificial marine water (AMW) [ASTM D1141-98 (Re-approved 2003)], simulating media usually used for ecotoxicological testing. A list of media composition is reported in Table A1-Annex.

Preparation of CuO samples in buffer solution

Buffer solution

The buffer solution was used to simulate the typical pH of the extracellular fluid (pH=7.4). The solution was prepared at a concentration of total phosphate equal to 0.05 M and with a molar ratio between the ionic species of $HPO_4^{2-}/H_2PO_4^-$ (61%/39%).

Capping agent solutions

10 ml of stock solution was prepared for each capping agent at 0.175 g/mL. Complete dissolution of the capping agents was obtained by mixing and, where necessary, by ultrasonication (Hielscher Ultrasonics GmbH, Germany). The capping agents used are:

- Na Citrate (CIT), MW 294,10, Aldrich
- Polyvinylpyrrolidone (PVP), MW 29000, Adrich
- Polyethylenimmine (PEI), MW 750000, Fluka
- Na ascorbate (ASC), MW 198,106, Riedel

Stock suspensions: CuO pristine and modified

CuO pristine stock suspension at a concentration of 10 g/L of Cu (1 wt%) was prepared dispersing CuO powder in buffer solution (total phosphate concentration: 0.05 M, pH=7.4). Starting from the stock suspension, modified CuO dispersions were prepared by adding 10 wt% of modifying agents (i.e. CIT, ASC, PEI and PVP) with respect to the total amount of copper oxide. This amount was estimated by stabilizers titration with electroacoustic technique (Acoustosizer, Colloidal Dynamics, USA). An amount of modifying agent equal to 10 wt% guarantees a complete covering on CuO NPs. Both pristine and modified stock suspension were mixed via ball milling (BM) process over 95 h with zirconia spheres (3 mm diameter). Five different stock suspensions were obtained after the ball milling process: pristine NPs (CuO-pristine), CuO NPs modified with sodium citrate (CuO-CIT), with sodium ascorbate (CuO-ASC), with polyethylenimine (CuO-PEI) and with polyvinylpyrrolidone (CuO-PVP).

Working stock suspensions: post grinding suspensions diluted in selected media

The grinding bodies are separated from each sample. Working stock suspension are prepared diluting samples in selected media, accordingly with concentration used in toxicological tests. The pH is measured after 24h, in order to allow for colloidal stabilization. Media and diluting condition considered in this experiment were:

- MilliQ water (100mg/L)
- DMEM added with Pyruvic acid and Pen-Strept and left at 37°C before dilution (50mg/L)
- MEM complete and left at 37°C before dilution (100mg/L)
- AFW/AMW (100 mg/L)

Characterization

A morphological characterization of pristine CuO NPs was performed by Scanning Transmission Electron Microscopy (STEM) analysis using Field Emission-Scanning Electron Microscopy (FE-SEM) instrument (Carl Zeiss Sigma NTS Gmbh, Oberkochen, DE). One drop of the different CuO NPs suspensions diluted in MilliQ water was deposited on a

film-coated copper grid and then dried at air. Particle size distribution was estimated by analyzing more than 50 particles. The hydrodynamic diameter was determined by DLS measurements, performed with a Zetasizer nano ZSP (model ZEN5600, Malvern Instruments, UK). Zeta potential measurements were performed by ELS technique. Smoluchowski equation was applied to convert the electrophoretic mobility to zeta potential. The pH measurements were performed on working stock suspensions after 24h in order to achieve the colloidal stabilization. Sedimentation velocity data of the colloidal dispersions were obtained from CSA, using the Multi-wavelength Dispersion Analyzer LUMiSizer 651®, based on STEPTM technology (space and time resolved extinction profiles), according to ISO/TR 13097:2013. The separation of different components in dispersion, performed by CSA, was speeded up by applying a Relative Centrifugal Force (RCF), which accelerates the movement of materials compared to gravity up to 2325 times. Sedimentation velocity data were calculated from the transmittance values obtained setting the wavelength of the transmitted light at 470 nm and selecting the transmittance (%) over time at three different positions (115, 120 and 125 mm far from the rotor) of the length of the cuvette. Sedimentation velocity at gravity was extrapolated after proving the linear dependency between RCF and sedimentation velocity at the RCF selected (2325).
Copper ions release was calculated as the ratio between dissolved copper ions and the total copper present in suspension. The quantification of copper ions dissolved in each medium was performed centrifuged 15 mL of each working stock suspension by Ultra-Centrifugal Filter (UCF) unit (Amicon Ultra-15, 10 kDa, Millipore), under centrifugal force of 5000 rpm and spin time of 30 min. The filtered solution (10 mL) was analyzed by inductively coupled plasma optical emission spectrometry using ICP-OES 5100 – vertical dual view apparatus (Agilent Technologies, Santa Clara, CA, USA). Total copper was quantified from each working stock suspension, which was previously treated with 2 mL of ultrapure HNO3 to ensure a complete digestion. According to experimental conditions typically of toxicological and ecotoxicological testing, the ions release experiments were performed at 37°C after 1 and 24 h in biological media and at 25°C in environmental media. The results from DLS, ELS, LUMiSizer and ICP-OES were reported as an average of three independent measurements.

Results and discussion

The morphological characterization of pristine CuO NPs by STEM analysis showed the presence of spherical and monodispersed CuO NPs (Fig. 1). The magnified image (Fig. 1b) highlights the presence of well dispersed NPs with a primary nanoparticle average diameter of about 12 ± 8 nm, according to supplier specification. As expected, some agglomerated NPs have also been detected (Fig. 1a and 1c).

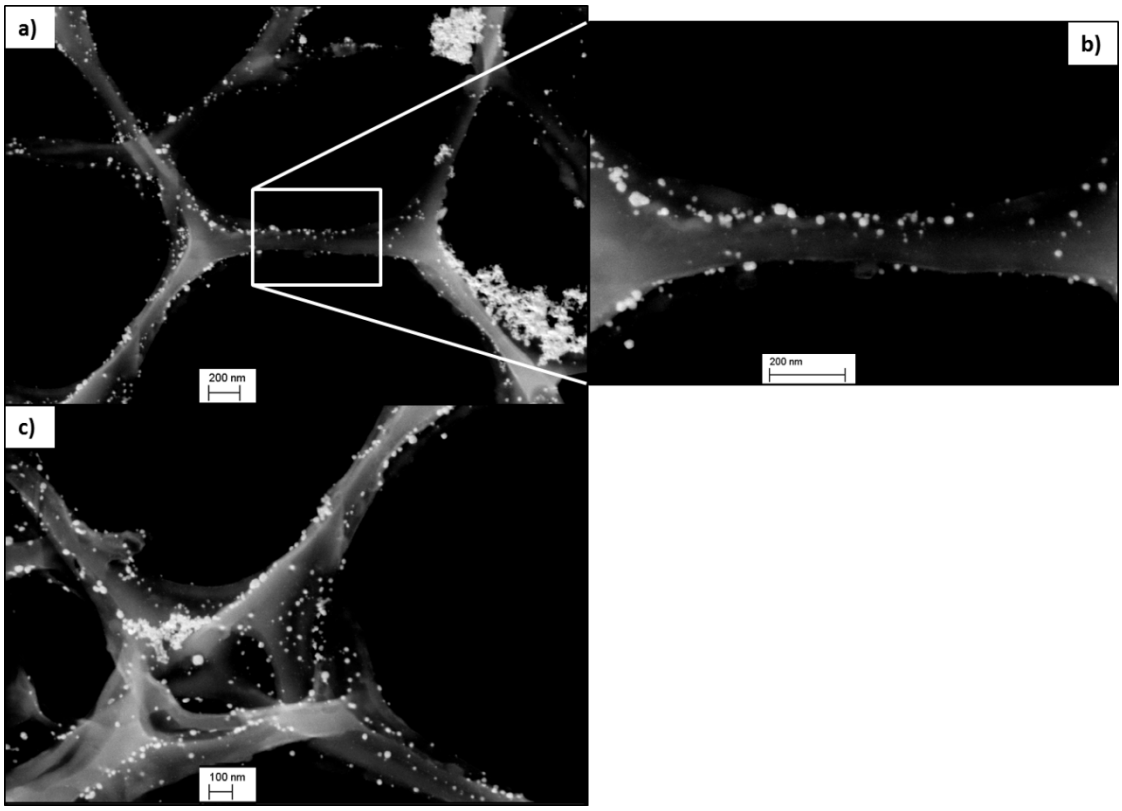

Figure 1 - STEM images of pristine CuO NPs (working suspension in MilliQ water).

DLS results, referred to pristine and modified CuO NPs diluted in MilliQ water, PBS, MEM, DMEM, AFW and AMW, are reported in Table 1.

Table 1. Hydrodynamic diameters (nm) of pristine and modified CuO samples dispersed in different media: MilliQ water, PBS, MEM, DMEM, AFW and AMW.

	Hydrodynamic Diameter (nm)					
	MilliQ	PBS	MEM	DMEM	AFW	AMW
CuO-pristine	1093 ± 50	2756 ± 347	47 ± 6	55 ± 16	1663 ± 210	1281 ± 393
CuO-CIT	368 ± 10	271 ± 43	89 ± 5	37 ± 2	1050 ± 16	1062 ± 159
CuO-ASC	122 ± 1.4	1314 ± 525	52 ± 4	73 ± 21	1293 ± 278	1234 ± 25
CuO-PEI	247 ± 14	209 ± 16	46 ± 4	45 ± 14	675 ± 199	1281 ± 168
CuO-PVP	797 ± 84	2765 ± 432	44 ± 2	53 ± 25	1159 ± 256	1661 ± 580

The data collected in MilliQ water confirmed the expected effect of surface modifiers addition. Samples coated by ionic agents (negative CIT and ASC, positive PEI) resulted better dispersed with a significant decreasing of average hydrodynamic diameter in comparison with pristine CuO NPs. On the other hand, neutral PVP did not improve significantly the dispersion of CuO NPs. The long aliphatic chains probably force NPs aggregation by depletion flocculation phenomenon (McFarlane NL et al., 2010) (Fig. 2b). In comparison with MilliQ water, data collected in PBS showed an increase of the hydrodynamic diameter for CuO-pristine as well as for CuO-ASC and CuO-PVP. This is correlated to aggregation phenomena and justified by the increase of ionic strength due to the salts content in PBS medium. It has already been reported that the salts screen the charge on the NP surface reducing electrostatic repulsion (Liu and Chen 2016). However, CuO-CIT and CuO-PEI modified samples were not affected by the presence of salts in

solution, showing hydrodynamic size values comparable with that measured in MilliQ water. From DLS measurements, CuO-PEI resulted the best dispersed in both MilliQ water and in a higher ionic strength medium (PBS). A possible explanation could be related to the electrosteric action of polyethylenimine (Karimi et al., 2012). The overall outcomes highlighted that ascorbate and citrate salts improved only the repulsive potential due to the negative charge transferred to particle surface, while PEI provides both electrostatic (due to positive charge) and steric contribution (due to the polymeric structure).
All DLS data collected in MEM and DMEM cell culture media showed very similar values. Biological components (amino acids and proteins) of the milieu seems to strongly levelled the hydrodynamic size data in spite of the stabilizers used. However, taking into account the samples dispersed in AFW and AMW, an increase of the hydrodynamic diameters was observed for both the pristine and modified NPs. The salts contained in environmental media, in particular divalent cations (e.g. Ca(II) and Mg(II)) that can get adsorbed to the nanoparticles surface, induced particles agglomeration. This phenomenon was already observed in AFW, which presents an ionic strength ten time lower than AMW. Agglomeration in AFW seems to be prevented only by PEI, which loses its efficacy in AMW at highest ionic strength (Mudunkotuwa and Grassian 2015).

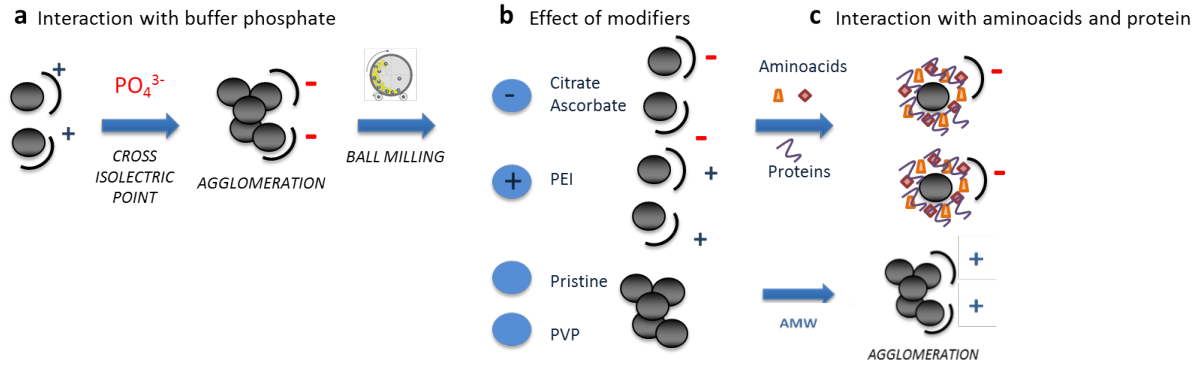

Figure 2 - Hypothetic scheme of the interactions between CuO NPs and different coatings

ζ-potentials of biological media were measured at around pH 8 and values of -9.9 ± 0.2 mV and -10.6 ± 0.3 mV were obtained for MEM and DMEM respectively. The results collected for pristine and the modified samples are listed in Table 2.

Table 2. ζ-potential (mV) of pristine and modified CuO samples dispersed in different media: MilliQ water, PBS, DMEM, MEM, AFW and AMW.

	ζ-pot (mV)					
	MilliQ (pH=6.5)	PBS (pH=7.4)	MEM (pH=7.9)	DMEM (pH=8.2)	AFW (pH=8.1)	AMW (pH=8.1)
CuO-pristine	-9.1 ± 0.4	-2.3 ± 2.1	-10.1 ± 0.5	-8.2 ± 0.4	-3.5 ± 0.4	+7.6 ± 0.4
CuO-CIT	-18.0 ± 0.3	-3.4 ± 1.2	-10.5 ± 0.2	-9.7 ± 0.6	-3.6 ± 0.4	+4.5 ± 0.7
CuO-ASC	-17.4 ± 0.3	-8.1 ± 0.1	-9.5 ± 0.2	-9.2 ± 0.2	-8.1 ± 0.4	+2.7 ± 0.6
CuO-PEI	+28.3 ± 0.7	+13.8 ± 0.1	-10.5 ± 0.9	-10.1 ± 0.7	+20.9 ± 0.9	+10.1 ± 1.1
CuO-PVP	-8.1 ± 2.3	-0.9 ± 0.7	-10.1 ± 0.4	- 9.4 ± 0.8	+1.6 ± 0.3	+6.5 ± 1.5

Pristine CuO NPs diluted in MilliQ water showed negative ζ-potential, despite to the expected positive value of copper oxide and in general of basic metal oxides when dispersed in water (Karlsson et al., 2013; Ji et al., 2010). The reversal of CuO pristine surface charge sign is due to the presence of phosphate ions (PO_4^{3-}) used for the sample preparation, which are specifically adsorbed onto CuO NPs surface. The key role of

phosphate adsorption has been already reported in literature (Liu and Chen 2016; Ji et al., 2010). The modified samples diluted in MilliQ water showed values coherent with the charge lead by the stabilizers, confirming the preferred interaction of aforementioned modifiers over phosphate ions (Fig. 2b). As expected, the addition of neutral PVP coating did not modify the ζ-potential of pristine sample. An increase of ionic strength induced a colloidal destabilization in PBS, as confirmed both by the increased agglomeration rate (Table 1) and by ζ-pot decrease (Table 2). ζ-pot values of CuO-pristine and CuO-PVP are close to zero, indicating the proximity to the isolectric point (pH_{IEP}). The coherence between NP size and ζ-pot results confirmed that DLS coupled with ELS represents an effective tool for the colloidal stability evaluation. As far as complete DMEM and MEM, ζ-pot data are leveled off on the value measured for the biological media without NPs (negative ζ-pot around -10 mV, see Table 2). This can be in accordance with the protein-corona theory, in which NPs are probably covered by proteins upon contact with a biological medium (Ji et al., 2010; Catalano et al., 2015). As a result, amino acids and proteins seemed to overwhelm the effects of surface-modifying agents driven the colloidal stability.

On the other hand, particles dispersed in AFW showed ζ-pot values similar to PBS while a slightly increase was observed when the stabilization was performed by polymers. According to the media preparation, the ionic strengths of AFW and PBS were comparable. Positive ζ-pot values were detected for all the samples dispersed in AMW. As already described in the literature, inorganic divalent cations seem to get adsorbed on the NPs surface and to control the electrical double layer formation. (Mudunkotuwa and Grassian 2015).

A hypothetic scheme on how the different coatings (i.e. phosphate ions, modifiers, amino acids and proteins) affect the colloidal stability (in terms of aggregation and surface charge) of pristine and CuO-modified NPs is reported in Fig. 2.

Colloidal stability was also investigated through CSA by means of LUMiSizer, calculating sedimentation velocity of the CuO NPs previously dispersed at 100 mg/L in MQ, PBS, MEM, DMEM, AFW and AMW. Figure 3 shows the average sedimentation velocity data for pristine and modified CuO NPs dispersed in the six different media selected, highlighting a correlation with the hydrodynamic diameter determined by DLS (Table 1).

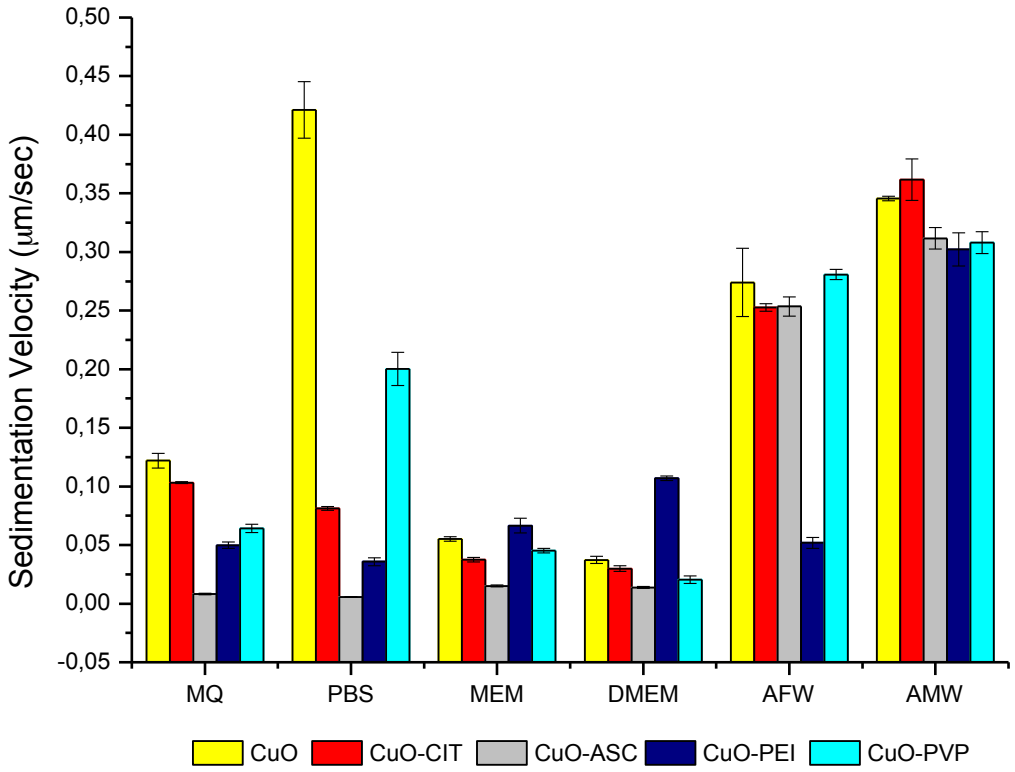

Figure 3 – Average sedimentation velocity data for pristine and modified CuO NPs dispersed in MilliQ, PBS, MEM, DMEM, AFW and AMW.

Sedimentation velocity distributions are reported in Figure 4. In general, it was confirmed that the modifying agents improved the colloidal stability of the dispersions, avoiding or decreasing the formation of CuO aggregates with respect to pristine CuO NPs. In particular, as far as MilliQ and PBS media, the sedimentation velocity distribution decreased for all the modified suspensions compared to pristine CuO NPs. The sedimentation velocity rate in these two aqueous media followed the same rank observed for hydrodynamic diameter data in MilliQ (Table 1), in which pristine and CuO-PVP suspensions are less stable than CuO-CIT followed by CuO-PEI and CuO-ASC. The correlation between LUMiSizer and DLS data was also noticed for CuO-pristine and CuO-PVP dispersed in PBS, showing both the highest sedimentation velocity values and agglomeration rates. Surprisingly, CuO-ASC dispersion revealed the lowest sedimentation velocity values in PBS but high average hydrodynamic diameter (> 1 µm). Taking into account the two different biological media, the results from LUM and DLS suggest that proteins and amino acids enhance the stability rate of the dispersions, both for pristine as well as for modified CuO. The only exception is represented by slightly higher sedimentation velocity values of CuO-PEI than the other dispersions. However, a more precise analysis of the sedimentation rates can be achieved by considering LUMiSizer numerical data thorough their quartiles, using box plot as a graphical descriptive statistic (Fig. 4). Knowledge on the degree of dispersions (spread), the skewness in the data and the outliers allow to achieve more accurate information on the colloidal stability of the different dispersions with respect to the DLS data previously obtained. For example, CuO-ASC, despite the high hydrodynamic diameter detected by DLS in PBS, shows a very narrow distribution of data (due to the homogeneity of the NPs) and in general the best

suspension stability in all the media analyzed. Finally, NPs dispersed in environmental media followed the same rank observed by DLS. An increase of instability

Conclusions

The general discussion and conclusions on STIS experiments are included in Deliverable 6.3 "Report on molecular, histological, biochemical and epigenetic responses as well as information on biopersistence identified in the STIS with pristine and released/aged NOAA".

3 Other characterization data for SUN samples in different media

Additional characterization of SUN samples has been performed in water and biological media. UoP studied dissolution rate, agglomeration and settling rate of pristine CuO NPs in Dechlorinated Plymouth City tapwater at pH 5, 6, 7. INIA determined shape (by TEM), particle size distribution (by DLS and/or TEM) and polydispersivity index (by DLS) of pristine CuO NPs, WCCo, MWCNTs, OrgPig and Fe_2O_3 in two biological media: 1) Leibovitz´s L-15 (Lonza; Cat nºBE12-700F) + 1% L-Gln + 1% Pen/Strep + 10% FBS; 2) EMEM (Lonza; Cat nº BE12-125F) + 1% L-Gln + 1% Pen/Strep + 1% non-essential amino acids + 10% FBS. Moreover, particle size distribution and polydispersivity index (by DLS) of modified CuO NPs with sodium citrate (CIT), sodium ascorbate (ASC), polyvinylpyrrolidone (PVP) and branched polyethylenimine (PEI) have been investigated in the same two biological media.

Characterization of pristine CuO NPs in Dechlorinated Plymouth City tapwater

CuO NPs were suspended in ultrapure water, dispersed in a sonic bath and then diluted into aquarium water. Plymouth City Tapwater was filtered (0.22 µm) and diluted 9 parts: 1 part with ultrapure water and after dilution was (in mM): Ca 0.37; K 0.04; Mg 0.08; Na 0.39. For characterisation, tapwater was diluted to pH 5, 6 and 7 with 0.2N HCl. The parameters, techniques and sample preparation conditions are synthetized in Table 23. Dissolution rates, hydrodynamic diameter and % Cu remained in suspension are collected in Table 24, 25 and 26. Data in Table 24 are based on measured concentrations of dissolved Cu species i.e. NPs are retained in dialysis tubing with respect to size. Concentration of NPs was not measured over time.

Table 23 – Parameters, techniques and sample preparation conditions.

Parameter	Technique	Sample type	Other
Dissolution rate	ICP-MS	10 mg/L Pristine CuO NPs tracked over 24 h	CuO NPs sonicated for 1 h in bath sonicator (FisherBrand Elmasonic S15, 95 W, 37 kHz)
Agglomeration rate	Nanoparticle Tracking Analysis	100 mg/L Pristine CuO NPs tracked over 24 h	CuO NPs sonicated for 1 h in bath sonicator (FisherBrand Elmasonic S15, 95 W, 37 kHz)
Settling rate	ICP-OES	100 mg/L Pristine CuO NPs tracked over 24 h	CuO NPs sonicated for 1 h in bath sonicator (FisherBrand Elmasonic S15, 95 W, 37 kHz)

Table 24 - % dissolution over 24 h of pristine CuO NPs in dechlorinated Plymouth tap water adjusted to pH 7, 6 and 5. Data are means (n=3) and standard deviations.

Time (h)	pH 7	pH 6	pH 5
0.5	0.011±0.017	0.005±0.001	0.002±0.004
1	0.05±0.002	0.174±0.003	1.296±0.09
2	0.087±0.007	0.298±0.011	2.285±0.155
3	0.105±0.01	0.355±0.017	2.171±0.135
6	0.135±0.02	0.428±0.039	3.089±0.094
12	0.147±0.02	0.485±0.055	3.963±0.098
24	0.171±0.028	0.603±0.078	5.01±0.086

Table 25 - Size in nm of CuO NPs (and homoagglomerates) at 0 h (after 15 min equilibration) and after 24 h in dechlorinated Plymouth tap water adjusted to pH 7, 6 and 5. Data are means (n=3) of normalised data and standard deviations.

Time (h)	pH 7	pH 6	pH 5
0	66±86	57±80	61±79
24	52±199	76±126	104±116

Table 26 - % Cu (i..e both dissolved and particulate Cu) remaining in suspension during 24 h in dechlorinated Plymouth tap water adjusted to pH 7, 6 and 5. Data are means (n=3) and standard deviations.

Time (h)	pH 7	pH 6	pH 5
0	100	100	100
1	76.20±2.71	45.13±1.75	59.48±10.22
3	17.50±2.19	18.08±0.69	36.61±7.82
6	7.57±0.62	6.02±0.66	19.18±2.77
24	1.56±0.45	1.09±0.06	3.37±0.76

The main comments are reported here below:

- Dissolution rate was higher at acid pH (Table 24)
- At time 0, CuO NPs in suspension were as individual particles or small agglomerates (Table 25). After 24 h, NPs in suspension were still largely individual particles or small agglomerates but a higher percentage of larger agglomerates was observed. This is refelected by the higher standard deviation at 24 than 0 h.
- Settling rate is slower at acid pH (Table 26), although this is based on total Cu remaining in suspension and data may therefore reflect higher rates of dissolution at pH 5 (see Table 24) and measurement of dissolved Cu species.
- Based on data in tables 25 and 26, suggestion is that CuO NPs agglomerate in dechlorinated tapwater and these agglomerates are probably not in suspension after 24 h.

Characterization of SUN samples in two biological media

NPs sample preparation in cell culture media (Leibovitz´s L-15 or EMEM supplemented medium)

All NP stocks in milli-Q water (except in the case of MWCNTs stock, see below) were prepared at the nominal concentration of 10 mg/ml, as follows:

> 50 mg of NP nanopowder were poured into a 10 ml Pyrex vial and the sample was wet with 100 µl of sterile milli-Q water, added drop by drop, allowing gentle tapping to ensure proper wetting of the sample (2 mins). Thereafter, 4.9 ml of sterile milli-Q water were added to obtain a 10 mg/ml stock dispersion.
> Probe (2mm) sonication was used to further disperse the stock suspension. The sonicator was set at 80% amplitude, "no pulse" (energy density delivered in 500 ml of ultrapure water: 16 J/mL approx.) and the tip was placed 2-2.5 cm into the vial containing the suspension, which was placed in an ice-water bath. The stock was then sonicated for 20 min.

To prepare the exposure dispersions in cell culture medium we firstly added a dispersant agent (BSA) to the stock solution, before mixing them with the biological medium, as it is detailed:

> In a 1.5 ml polypropylene tube, we added 25 µl of a 80 g/l BSA solution to 75 µl of the stock suspension, to obtain an intermediate nanomaterial dispersion. This was transferred into a 10 ml glass vial containing 7.4 ml of L-15 or EMEM supplemented medium (Leibovitz´s L-15 + 1% L-Gln + 1% Pen/Strep + 10% FBS or EMEM + 1% L-Gln + 1% Pen/Strep + 1% non-essential amino acids + 10% FBS), to yield the highest exposure concentration of 100 µg/ml of nanomaterial. The obtained dispersion was stirred by using vortex for 5 seconds, and afterwards sonicated in a bath sonicator (37 KHz) for 10 minutes. The resulting suspension was used as quick as possible for in vitro toxicological testing and/or for Dynamic Light Scattering (DLS) analysis. For TEM analyses, the NP suspensions were prepared at a nominal concentration of 200 µg/ml. In this case, the volumes used were: 50 µl of 80 g BSA /l solution, 150 µl of the NP stock in water (at 10 mg/ml) and 7.3 ml of cell culture medium.

For MWCNTs the concentration of the stock was reduced to ¼ (2.5 mg/ml) to obtain a more easy to handle dispersion, since at higher concentration, the suspension obtained after probe sonication was too thick to work with. The MWCNTs stock in milli-Q water was prepared in the same way as described above, but mixing 12.5 mg (instead 50 mg) of nanotubes powder with 5 ml of milli-Q water, to yield a stock concentration of 2.5 mg/ml (instead of 10 mg/ml). To obtain the highest exposure dispersion in biological medium at the same concentration of MWCNTs as the rest of NPs (100 µg/ml), the volume of the stock mixed with the 25 µl of BSA was 300 µl (instead 75 µl), and this intermediate dispersion was added to 7.175 ml of L-15 or EMEM supplemented medium. This dispersion (at 100 µg/ml) was used for in vitro toxicological testing and /or for DLS analysis. For TEM analyses, the MWCNTs dispersions at 100 µg/ml were serially ½ diluted in cell culture medium to obtain a final concentration of 12.5 µg/ml, to allow us to distinguish discrete MWCNTs particles in the micrographs.

Pristine CuO NPs in Leibovitz´s L-15 (Lonza; Cat nºBE12-700F) + 1% L-Gln + 1% Pen/Strep + 10% FBS

Shape and size distribution of CuO NPs in Leibovitz´s L-15 (Lonza; Cat nºBE12-700F) + 1% L-Gln + 1% Pen/Strep + 10% FBS obtained by TEM are depicted in Figures 5 and 6 respectively. Table 27 shows the characterization data of pristine CuO NPs in the cell culture medium.
Samples for TEM analysis were prepared in two-fold concentration (200 µg/mL) in cell culture medium, respect to that used for cell exposure (100 µg/mL) and DLS analyses, to make easier finding NPs images along the grids. Size distributions of the most concentrated NPs dispersions were similar to those obtained by the 100 µg/mL dispersions by DLS means.

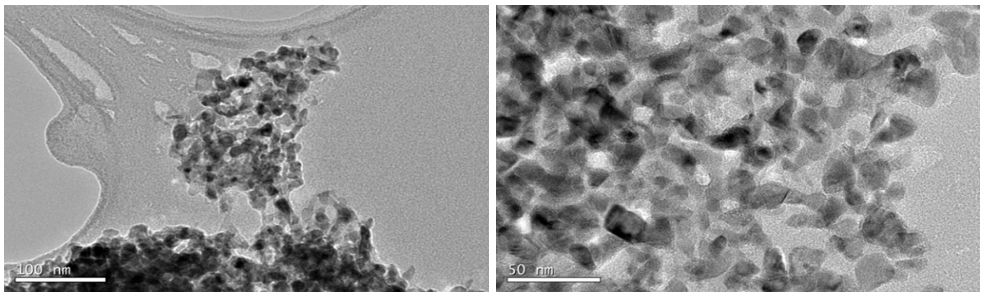

Figure 5 - Shape (TEM) of NPs dispersions in cell culture medium (at 200 µg/mL).

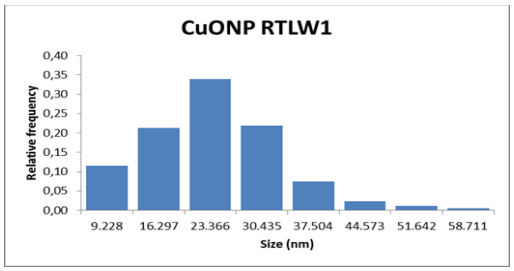

Figure 6 - Size distribution (TEM) of NPs dispersions in cell culture medium (at 200 µg/mL).

Table 27 – Hydrodynamic diameter of CuO NPs in the cell culture medium tested. Blue values refer to L-15 medium+ supplements with BSA and without NPs.

Nanoparticle	Z-aver and PSD (Mean dm in nm ± SEM) Time: 0 h	PdI Time: 0 h	Z-aver and PSD (Mean dm in nm ± SEM) Time: 24 h	PdI Time: 24 h
CuO NPs	130.98 ± 7.17 201.23 ± 15.10 (88%) 19.24 ± 1.95 (5%) 4679.31 ± 121.20 (7%)	0.57 ± 0.09	40.11 ± 10.23 45.49 ± 6.23 (44%) 405.56 ± 111.77 (30%) 10.01 ± 0.49 (26%)	0.53 ± 0,08

Hydrodynamic size distribution (Table 27) evidences that CuO NPs are unstable in suspension as they agglomerate and/or de-agglomerate or dissolve after 24 hours of incubation in L-15 medium+ supplements at 20° C. DLS main peak in fresh preparations disappear after 24 h of incubation, and two new peaks with a smaller and a bigger sizes appear. Values in blue also appear in L-15 medium+ supplements with BSA and without NPs. CuO NPs appear in TEM images as agglomerates in fresh L-15 medium+ supplements dispersions. Individual CuO NPs have a near-spherical shape. Size of individual NPs along the agglomerates has been calculated. Peaks obtained by DLS analyses may correspond to CuO NPs agglomerates.

Pristine WCCo NPs in Leibovitz´s L-15 (Lonza; Cat nºBE12-700F) + 1% L-Gln + 1% Pen/Strep + 10% FBS

Shape and size distribution of WCCo NPs in Leibovitz´s L-15 (Lonza; Cat nºBE12-700F) + 1% L-Gln + 1% Pen/Strep + 10% FBS obtained by TEM are depicted in Figures 7 and 8 respectively. Table 28 shows the characterization data of pristine WCCo NPs in the cell culture medium.
Samples for TEM analysis were prepared in two-fold concentration (200 µg/mL) in cell culture medium, respect to that used for cell exposure (100 µg/mL) and DLS analyses, to make easier finding NPs images along the grids. Size distributions of the most concentrated NPs dispersions were similar to those obtained by the 100 µg/mL dispersions by DLS means.

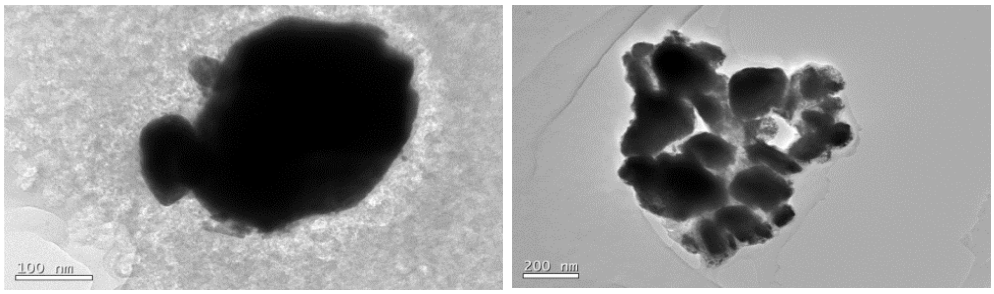

Figure 7 - Shape (TEM) of NPs dispersions in cell culture medium (at 200 µg/mL).

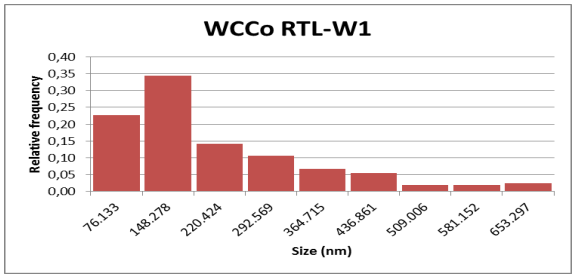

Figure 8 - Size distribution (TEM) of NPs dispersions in cell culture medium (at 200 µg/mL).

Table 28 - Hydrodynamic diameter of WCCo NPs in the cell culture medium tested.

Nanoparticle	Z-aver (Mean dm in nm ± SEM) Time: 0 h	PdI Time: 0 h	Z-aver (Mean dm in nm ± SEM) Time: 24 h	PdI Time: 24 h
WCCo NPs	419.32 ± 77.08	0.31 ± 0.09	373.00 ± 49.95	0.38 ± 0.08

WCCo NPs were well dispersed in L-15 medium+ supplements and the dispersions were stable over 24 hours at 20° C. TEM images of fresh WCCo NPs dispersions in L-15 medium+ supplements showed that NPs had a variable size and shape (from polyhedral to semi-spherical).

Pristine MWCNTs in Leibovitz´s L-15 (Lonza; Cat nºBE12-700F) + 1% L-Gln + 1% Pen/Strep + 10% FBS

Shape of MWCNTs in Leibovitz´s L-15 (Lonza; Cat nºBE12-700F) + 1% L-Gln + 1% Pen/Strep + 10% FBS obtained by TEM are depicted in Figure 9. Table 29 shows the characterization data of pristine MWCNTs in the cell culture medium.
MWCNTs samples for TEM are prepared at 12.5 µg/mL in cell culture medium, instead at 100 µg/mL (the highest concentration used for cell exposure and DLS analyses), to allow to distinguish discrete MWCNTs particles in the micrographs.

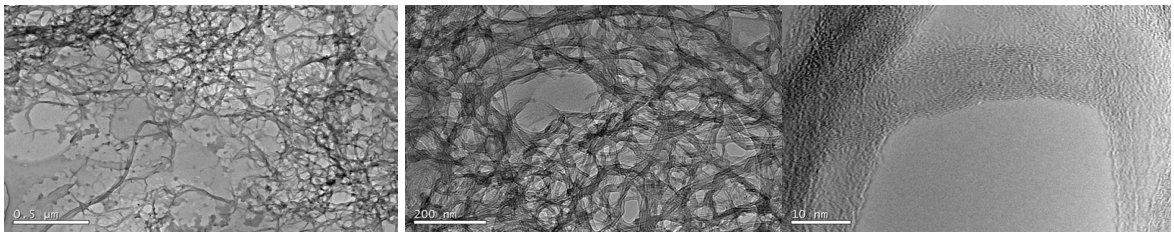

Figure 9 – Shape of MWCNTs dispersions in cell culture medium (12.5 µg/mL).

Table 29 - Particle size distribution of MWCNTs dispersions in cell culture medium (at 100 µg/mL). Blue values refer to L-15 medium+ supplements with BSA and without MWCNTs.

Nanoparticle	Z-aver and PSD (Mean dm in nm ± SEM) Time: 0 h	PdI Time: 0 h	Z-aver and PSD (Mean dm in nm ± SEM) Time: 24 h	PdI Time: 24 h
MWCNTs	612.33 ± 111.29 725.13 ± 57.01 (77%) 163.31 ± 19.30 (12%) 4848.25 ± 149.48 (11%)	0.51 ± 0.08	528.76 ± 112.91 652.96 ± 116.92 (85%) 141.92 ± 34.84 (7%) 4229.61 ± 548.81 (8%)	0.44 ± 0.02

MWCNTs yielded a polydisperse pattern by DLS means, due to the fact that MWCNTs do not have a spherical shape. However, at 100 µg/mL, their size distribution remained stable over 24 hours in L-15 medium+ supplements at 20° C. Values in blue also appear in L-15 medium+ supplements with BSA and without MWCNTs. TEM images of fresh MWCNTs dispersions in L-15 medium+ supplements show brunches of nanotubes and a MWCNT diameter of about 10 nm.

Pristine Organic Pigment RED 254 NPs in Leibovitz´s L-15 (Lonza; Cat nºBE12-700F) + 1% L-Gln + 1% Pen/Strep + 10% FBS

Shape and size distribution of Organic Pigment RED 254 NPs in Leibovitz´s L-15 (Lonza; Cat nºBE12-700F) + 1% L-Gln + 1% Pen/Strep + 10% FBS obtained by TEM are depicted in Figure 10 and 11 respectively. Table 30 shows the characterization data of pristine NPs in the cell culture medium.
Samples for TEM are prepared in two-fold concentration (200 µg/mL) in cell culture medium, respect to that used for cell exposure (100 µg/mL) and DLS analyses, to make easier finding NPs images along the grids. Size distributions of the most concentrated NPs dispersions are similar to those obtained by the 100 µg/mL dispersions by DLS means.

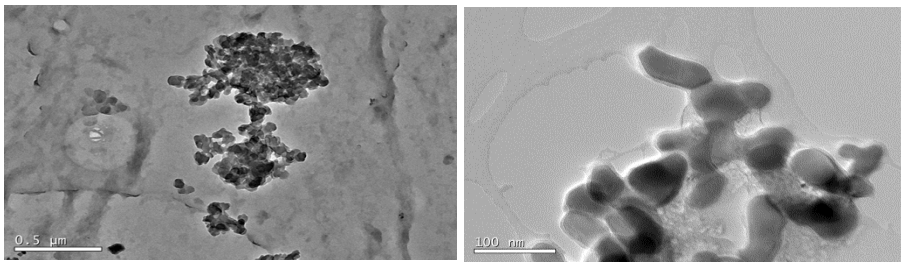

Figure 10 - Shape (TEM) of NPs dispersions in cell culture medium (at 200 µg/mL).

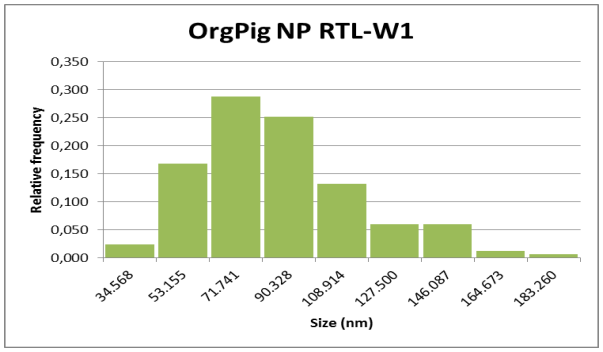

Figure 11 - Size distribution (TEM) of NMs dispersions in cell culture medium (at 200 µg/mL).

Table 30 - Particle size distribution of NPs dispersions in cell culture medium (at 100 µg/mL).

Nanoparticle	Z-aver (Mean dm in nm ± SEM) Time: 0 h	PdI Time: 0 h	Z-aver (Mean dm in nm ± SEM) Time: 24 h	PdI Time: 24 h
OrgPig Red254	193.62 ± 7.13	0.24 ± 0.02	193.44 ± 7.71	0.24 ± 0.03

OrgPig Red254 NPs were well dispersed in L-15 medium+ supplements and OrgPigRed254 dispersions were stable for 24 hours at 20° C. TEM images of fresh OrgPig Red 254 dispersions in L-15 medium+ supplements showed that NPs aggregate and individual NPs had a rod-like shape. Peaks detected by DLS may correspond to OrgPigRed254 agglomerates, since individual NPs diameter calculated by TEM have a smaller size than that stimated by DLS.

Pristine Fe_2O_3 NPs in Leibovitz´s L-15 (Lonza; Cat nºBE12-700F) + 1% L-Gln + 1% Pen/Strep + 10% FBS

Shape and size distribution of Fe_2O_3 NPs in Leibovitz´s L-15 (Lonza; Cat nºBE12-700F) + 1% L-Gln + 1% Pen/Strep + 10% FBS obtained by TEM are depicted in Figure 12 and 13 respectively. Table 31 shows the characterization data of pristine NPs in the cell culture medium.
Samples for TEM are prepared in two-fold concentration (200 µg/mL) in cell culture medium, respect to that used for cell exposure (100 µg/mL) and DLS analyses, to make easier finding NPs images along the grids. Size distributions of the most concentrated NPs dispersions are similar to those obtained by the 100 µg/mL dispersions by DLS means.

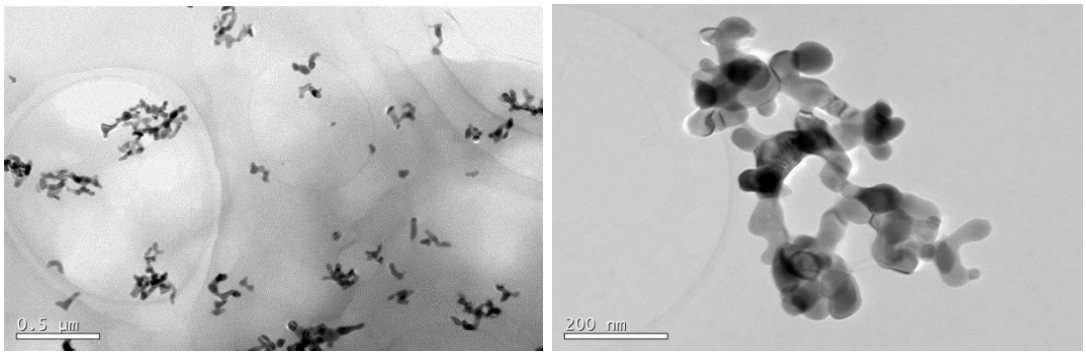

Figure 12 – Shape (TEM) of Fe_2O_3 NPs dispersions in cell culture medium (at 200 µg/mL).

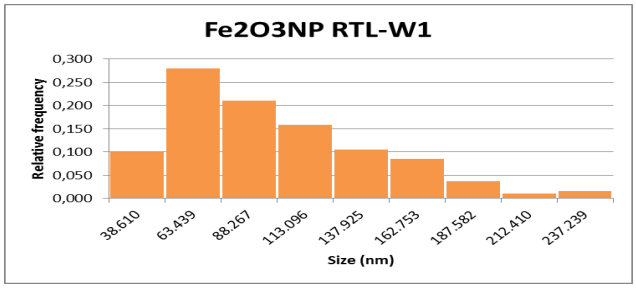

Figure 13 - Size distribution (TEM) of Fe_2O_3 NPs dispersions in cell culture medium (at 200 µg/mL).

Table 31 - Particle size distribution of Fe_2O_3 NPs dispersions in cell culture medium (at 100 µg/mL).

Nanoparticle	Z-aver (Mean dm in nm ± SEM) Time: 0 h	PdI Time: 0 h	Z-aver (Mean dm in nm ± SEM) Time: 24 h	PdI Time: 24 h
PigRed101 NPs	210.28 ± 6.34	0.15 ± 0.02	212.13 ± 7.06	0.13 ± 0.01

Fe_2O_3 NPs were well dispersed in L-15 medium+ supplements and the dispersions were stable for 24 hours at 20° C. TEM images of fresh Fe_2O_3 NPs dispersions in L-15 medium+ supplements showed that individual NPs had a smaller size than that stimated by DLS and they have a rod-like shape. Size of individual NPs along the agglomerates has been calculated. Peaks obtained by DLS analysis may correspond to Fe_2O_3 NPs agglomerates.

CuO_101 NPs in Leibovitz´s L-15 (Lonza; Cat nºBE12-700F) + 1% L-Gln + 1% Pen/Strep + 10% FBS

Table 32 shows the characterization data of CuO_101 NPs (96 h ball milling in phosphate buffer) in the cell culture medium.

Table 32 - Particle size distribution of CuO_101 NPs dispersions in cell culture medium (at 100 µg/mL). Blue values refer to L-15 medium+ supplements with BSA and without NPs.

Nanoparticle	Z-aver and PSD (Mean dm in nm ± SEM) Time: 0 h	PdI Time: 0 h	Z-aver and PSD (Mean dm in nm ± SEM) Time: 24 h	PdI Time: 24 h
CuONP_101	46.39 ± 9.50 129.07 ± 5.72 (74%) 10.19 ± 0.56 (20%) 4241.56 ± 103.83 (7%)	0.62 ± 0.04	22.24 ± 2.20 169.79 ± 67.43 (47%) 12.32 ± 1.01 (45%) 4909.92 ± 179.48 (8%)	0.73 ± 0.08

Hydrodynamic size distribution evidences that ball milled CuO_101 NPs were stable in suspension along 24 hours in L-15 medium+ supplements at 20° C. However, since percentage of intensity of the main peak decreases, CuO_101 NPs might precipitate or dissolve along this time. Values in blue also appear in L-15 medium+ supplements with BSA and without NPs.

CuO-CIT NPs in Leibovitz´s L-15 (Lonza; Cat nºBE12-700F) + 1% L-Gln + 1% Pen/Strep + 10% FBS

Table 33 shows the characterization data of CuO-CIT NPs in the cell culture medium.

Table 33 - Particle size distribution of CuO-CIT NPs dispersions in cell culture medium (at 100 µg/mL). Blue values refer to L-15 medium+ supplements with BSA and without NPs.

Nanoparticle	Z-aver and PSD (Mean dm in nm ± SEM) Time: 0 h	PdI Time: 0 h	Z-aver and PSD (Mean dm in nm ± SEM) Time: 24 h	PdI Time: 24 h
CuONP_102	41.38 ± 10.06 112.65 ± 11.65 (75%) 10.15 ± 0.52 (23%) 4422.44 ± 98.07 (2%)	0.62 ± 0.02	18.34 ± 0.38 68.94 ± 11.58 (33%) 14.83 ± 1.28 (64%) 3626.22 ± 987.66 (3%)	0.43 ± 0.02

Hydrodynamic size distribution (DLS) evidences that CuO-CIT NPs may dissolve and/or de-

aggregate after 24 hours of incubation at 20° C in L-15 medium+ supplements, since size and intensity of the main peak detected by DLS decreases. Values in blue also appear in L-15 medium+ supplements with BSA and without NPs.

CuO-PEI NPs in Leibovitz´s L-15 (Lonza; Cat nºBE12-700F) + 1% L-Gln + 1% Pen/Strep + 10% FBS

Table 34 shows the characterization data of CuO-PEI NPs in the cell culture medium.

Table 34 - Particle size distribution of CuO-PEI NPs dispersions in cell culture medium (at 100 µg/mL). Blue values refer to L-15 medium+ supplements with BSA and without NPs.

Nanoparticle	Z-aver and PSD (Mean dm in nm ± SEM) Time: 0 h	PdI Time: 0 h	Z-aver and PSD (Mean dm in nm ± SEM) Time: 24 h	PdI Time: 24 h
CuONP_104	270.96 ± 128.19 445.20 ± 48.80 (78%) 84.54 ± 30.19 (12%) 14.07 ± 3.86 (10%)	0.75 ± 0.14	133.76 ± 75.82 392.74 ± 62.72 (48%) 34.90 ± 1.91 (21%) 11.21 ± 1.37 (31%)	0.69 ± 0.12

Hydrodynamic size distribution (DLS) evidences that CuO-PEI NPs may dissolve and/or de-aggregate (at least in part) in suspension in L-15 medium+ supplements since a new smaller peak appears after 24 h of incubation at 20° C. Values in blue also appear in L-15 medium+ supplements with BSA and without NPs.

CuO-ASC NPs in Leibovitz´s L-15 (Lonza; Cat nºBE12-700F) + 1% L-Gln + 1% Pen/Strep + 10% FBS

Table 35 shows the characterization data of CuO-ASC NPs in the cell culture medium.

Table 35 - Particle size distribution of CuO-ASC NPs dispersions in cell culture medium (at 100 µg/mL). Blue values refer to L-15 medium+ supplements with BSA and without NPs.

Nanoparticle	Z-aver and PSD (Mean dm in nm ± SEM) Time: 0 h	PdI Time: 0 h	Z-aver and PSD (Mean dm in nm ± SEM) Time: 24 h	PdI Time: 24 h
CuONP_105	40.51 ± 0.13 119.38 ± 1.05 (75%) 12.46 ± 1.33 (24%) 4654.67 ± 36.83 (1%)	0.58 ± 0.02	18.35 ± 1.56 16.35 ± 4.03 (71%) 52.51 ± 6.03 (21%) 2995.41 ± 1114.16 (8%)	0.44 ± 0.11

Hydrodynamic size distribution (DLS) evidences that CuO-ASC may dissolve and/or de-aggregate in suspension in L-15 medium+ supplements since the principal peak that is present in fresh preparations completely dissapeared, and a new smaller peak appeared (with less intensity frequency) after 24 h of incubation at 20° C. Values in blue also appeared in L-15 medium+ supplements with BSA and without NPs.

Pristine CuO NPs in EMEM (Lonza; Cat nº BE12-125F) + 1% L-Gln + 1% Pen/Strep + 1% non-essential amino acids + 10% FBS

Shape of CuO NPs in EMEM (Lonza; Cat nº BE12-125F) + 1% L-Gln + 1% Pen/Strep + 1% non-essential amino acids + 10% FBS obtained by TEM is depicted in Figure 14. Table 36 shows the

characterization data of pristine CuO NPs in the cell culture medium.
Samples for TEM are prepared in two-fold concentration (200 µg/mL) in cell culture medium, respect to that used for cell exposure (100 µg/mL) and DLS analyses, to make easier finding NPs images along the grids. Size distributions of the most concentrated NPs dispersions are similar to those obtained by the 100 µg/mL dispersions by DLS means.

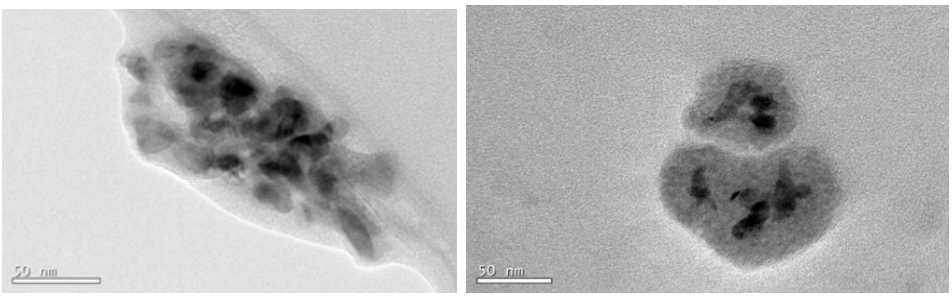

Figure 14 - Shape (TEM) of NPs dispersions in cell culture medium (at 200 µg/mL).

Table 36 - Particle size distribution of NPs dispersions in cell culture medium (at 100 µg/mL). Blue values refer to L-15 medium+ supplements with BSA and without NPs.

Nanoparticle	Z-aver and PSD (Mean dm in nm ± SEM) Time: 0 h	PdI Time: 0 h	Z-aver and PSD (Mean dm in nm ± SEM) Time: 24 h	PdI Time: 24 h
CuO NPs	134 ± 17.77 202.99 ± 17.14 (90%) 8.51 ± 0.75 (4%) 4581.75 ± 401.75 (6%)	0.49 ± 0.05	71.61 ± 34.56 214.97 ± 52.08 (46%) 11.45 ± 2.26 (40%) 42.86 ± 1.44 (14%)	0.63 ± 0.18

Hydrodynamic size distribution (DLS) evidences that CuO NPs were stable along 24 hours in EMEM medium + supplements since main peak size was maintained. Values in blue also appeared in EMEM medium+ supplements with BSA and without NPs. CuO NPs appeared in TEM images as agglomerates sourrounded by a non-identified material in fresh EMEM medium dispersions and after 24 hours of incubation at 28 °C. Individual CuO nanoparticles had a near-spherical shape. Peaks obtained by DLS analyses may correspond to CuO NPs agglomerates.

Pristine WCCo NPs in EMEM (Lonza; Cat nº BE12-125F) + 1% L-Gln + 1% Pen/Strep + 1% non-essential amino acids + 10% FBS

Shape of WCCo NPs in EMEM (Lonza; Cat nº BE12-125F) + 1% L-Gln + 1% Pen/Strep + 1% non-essential amino acids + 10% FBS obtained by TEM is depicted in Figure 15. Table 37 shows the characterization data of pristine CuO NPs in the cell culture medium.
Samples for TEM are prepared in two-fold concentration (200 µg/mL) in cell culture medium, respect to that used for cell exposure (100 µg/mL) and DLS analyses, to make easier finding NPs images along the grids. Size distributions of the most concentrated NPs dispersions are similar to those obtained by the 100 µg/mL dispersions by DLS means.

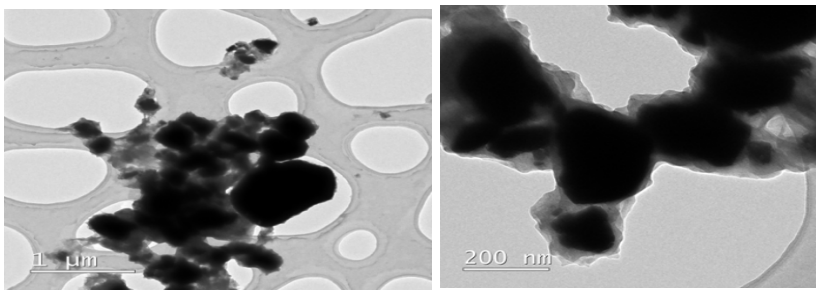

Figure 15 – - Shape (TEM) of NPs dispersions in cell culture medium (at 200 µg/mL).

Table 37 - Particle size distribution of NPs dispersions in cell culture medium (at 100 µg/mL).

Nanoparticle	Z-aver (Mean dm in nm ± SEM) Time: 0 h	PdI Time: 0 h	Z-aver (Mean dm in nm ± SEM) Time: 24 h	PdI Time: 24 h
WCCo NPs	276.30 ± 14.91	0.22 ± 0.01	227.96 ± 11.42	0.22 ± 0.02

Hydrodynamic size distribution (DLS) evidences that WCCo NPs were stable in EMEM medium+ supplements since peak pattern was maintained after 24 hours of incubation at 28° C, although a little reduction in size diameter was observed along this time, maybe due to a de-agglomeration and/or dissolving events. TEM images of fresh WCCoNPs dispersions in EMEM medium+ supplements showed that nanoparticles have a variable size and shape (from polyhedral to semi-spherical) and form agglomerates.

Pristine MWCNTs in EMEM (Lonza; Cat n° BE12-125F) + 1% L-Gln + 1% Pen/Strep + 1% non-essential amino acids + 10% FBS

Shape of MWCNTs in EMEM (Lonza; Cat n° BE12-125F) + 1% L-Gln + 1% Pen/Strep + 1% non-essential amino acids + 10% FBS obtained by TEM is depicted in Figure 16. Table 38 shows the characterization data of pristine CuO NPs in the cell culture medium.
MWCNTs samples for TEM are prepared at 12.5 µg/mL in cell culture medium, instead at 100 µg/mL (the highest concentration used for cell exposure and DLS analyses), to allow to distinguish discrete MWCNTs particles in the micrographs.

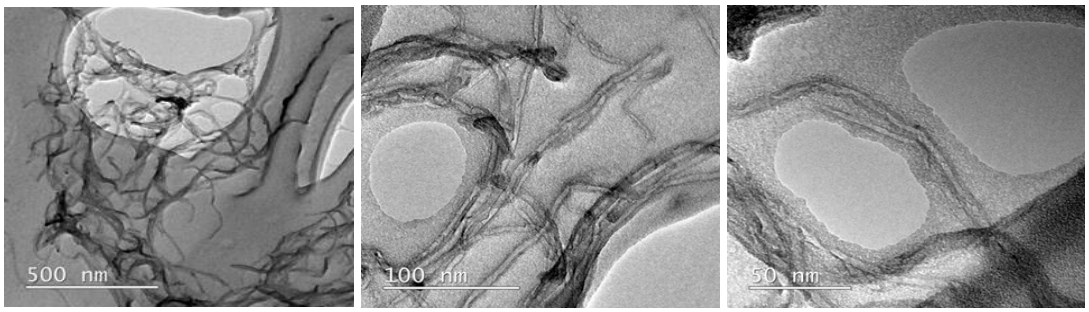

Figure 16 - Shape (TEM) of NMs dispersions in cell culture medium (at 200 µg/mL).

Table 38 - Particle size distribution of MWCNTs dispersions in cell culture medium (at 100 µg/mL). Blue values refer to L-15 medium+ supplements with BSA and without NPs.

Nanoparticle	Z-aver and PSD (Mean dm in nm ± SEM) Time: 0 h	PdI Time: 0 h	Z-aver and PSD (Mean dm in nm ± SEM) Time: 24 h	PdI Time: 24 h
MWCNTs	632.56 ± 133.62 657.08 ± 4.11 (90%) 107.03 ± 6.51 (5%) 4867.56 ± 98.94 (5%)	0.48 ± 0.07	723.75 ± 184.89 855.09 ± 116.62 (81%) 202.44 ± 38.15 (15%) 4930.33 ± 219.00 (4%)	0.59 ± 0.12

MWCNTs yielded a polydisperse pattern by DLS means, due to the fact that MWCNTs do not have a spherical shape. After 24 hours of incubation at 28° C, MWCNTs partially agglomerated as peak sizes increase along the time. Values in blue also appeared in EMEM medium+ supplements with BSA and without NPs. TEM images of fresh MWCNTs dispersions in EMEM medium+ supplements showed brunches of nanotubes and a MWCNT diameter of about 10 nm.

Pristine Organic Pigment RED 254 NPs in EMEM (Lonza; Cat n° BE12-125F) + 1% L-Gln + 1% Pen/Strep + 1% non-essential amino acids + 10% FBS

Shape and size distribution of Organic Pigment RED 254 NPs in EMEM (Lonza; Cat n° BE12-125F) + 1% L-Gln + 1% Pen/Strep + 1% non-essential amino acids + 10% *FBS* obtained by TEM is depicted in Figure 17. Table 39 shows the characterization data of pristine NPs in the cell culture medium.
Samples for TEM are prepared in two-fold concentration (200 µg/mL) in cell culture medium, respect to that used for cell exposure (100 µg/mL) and DLS analyses, to make easier finding NPs images along the grids. Size distributions of the most concentrated NPs dispersions are similar to those obtained by the 100 µg/mL dispersions by DLS means.

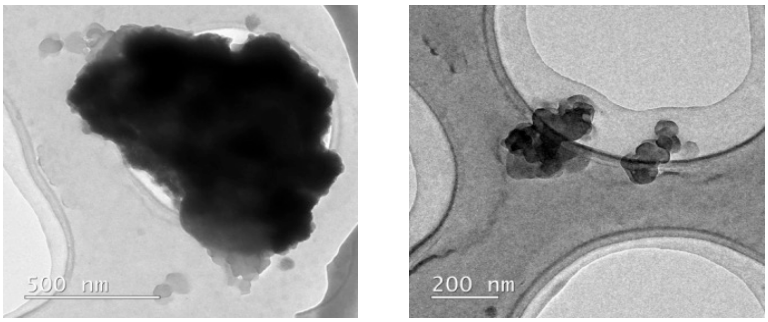

Figure 17 - Shape (TEM) of NMs dispersions in cell culture medium (at 200 µg/mL).

Table 39 - Particle size distribution of NPs dispersions in cell culture medium (at 100 µg/mL).

Nanoparticle	Z-aver (Mean dm in nm ± SEM) Time: 0 h	PdI Time: 0 h	Z-aver (Mean dm in nm ± SEM) Time: 24 h	PdI Time: 24 h
OrgPig Red254	196.01 ± 6.12	0.25 ± 0.01	196.33 ± 9.56	0.23 ± 0.04

OrgPig Red 254 NPs were well dispersed in EMEM medium+ supplements and the dispersions were stable for 24 hours at 28° C. TEM images of fresh OrgPig Red 254 dispersions in EMEM medium+ supplements showed that individual nanoparticles had near-spherical shape and they formed aggregates. Peaks obtained by DLS analyses may correspond to NPs agglomerates.

Fe_2O_3 NPs in EMEM (Lonza; Cat n° BE12-125F) + 1% L-Gln + 1% Pen/Strep + 1% non-essential amino acids + 10% FBS

Shape and size distribution of Fe_2O_3 NPs in EMEM (Lonza; Cat n° BE12-125F) + 1% L-Gln + 1% Pen/Strep + 1% non-essential amino acids + 10% *FBS* obtained by TEM is depicted in Figure 18. Table 40 shows the characterization data of pristine NPs in the cell culture medium.
Samples for TEM are prepared in two-fold concentration (200 µg/mL) in cell culture medium, respect to that used for cell exposure (100 µg/mL) and DLS analyses, to make easier finding NPs images along the grids. Size distributions of the most concentrated NPs dispersions are similar to those obtained by the 100 µg/mL dispersions by DLS means.

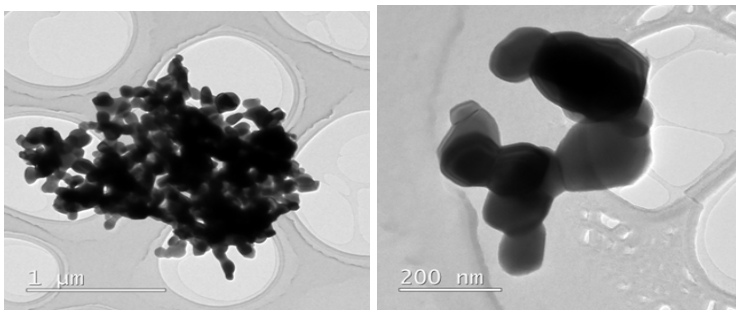

Figure 18 - Shape (TEM) of NMs dispersions in cell culture medium (at 200 µg/mL).

Table 40 - Particle size distribution of NPs dispersions in cell culture medium (at 100 µg/mL).

Nanoparticle	Z-aver and PSD (Mean dm in nm ± SEM) Time: 0 h	PdI Time: 0 h	Z-aver and PSD (Mean dm in nm ± SEM) Time: 24 h	PdI Time: 24 h
Fe_2O_3PigRed101	253.02 ± 20.19	0.21 ± 0.03	257.22 ± 25.78	0.20± 0.04

Fe_2O_3 NPs were well dispersed in EMEM medium+ supplements and the dispersions were stable for 24 hours at 28° C. TEM images of fresh dispersions in EMEM medium+ supplements showed Fe2O3 NPs aggregates and a rod-like shape.

CuO_101 NPs in EMEM (Lonza; Cat n° BE12-125F) + 1% L-Gln + 1% Pen/Strep + 1% non-essential amino acids + 10% FBS

Table 41 shows the characterization data of CuO_101 NPs in the cell culture medium.

Table 41 - Particle size distribution of NPs dispersions in cell culture medium (at 100 µg/mL). Blue values refer to EMEM medium+ supplements with BSA and without NPs.

Nanoparticle	Z-aver and PSD (Mean dm in nm ± SEM) Time: 0 h	PdI Time: 0 h	Z-aver and PSD (Mean dm in nm ± SEM) Time: 24 h	PdI Time: 24 h
CuONP_101	162.12 ± 5.60 236.8 ± 27.42 (97%) 4655.33 ± 38.10 (3%)	0.34 ± 0.07	121.70 ± 36.74 138.88 ± 3.10 (76%) 11.55 ± 0.59 (22%) 4655.00 ± 308.73 (2%)	0.39 ± 0.13

Hydrodynamic size distribution (DLS) evidences that CuO_101 NPs may dissolve or/and de-aggregate (since DLS main peak size decreases) after 24 hours of incubation at 28° C in EMEM medium+ supplements. Values in blue also appear in EMEM medium+ supplements with BSA and without NPs.

CuO-CIT NPs in EMEM (Lonza; Cat n° BE12-125F) + 1% L-Gln + 1% Pen/Strep + 1% non-essential amino acids + 10% FBS

Table 42 shows the characterization data of CuO-CIT NPs in the cell culture medium.

Table 42 - Particle size distribution of NPs dispersions in cell culture medium (at 100 µg/mL). Blue values refer to EMEM medium+ supplements with BSA and without NPs.

Nanoparticle	Z-aver and PSD (Mean dm in nm ± SEM) Time: 0 h	PdI Time: 0 h	Z-aver and PSD (Mean dm in nm ± SEM) Time: 24 h	PdI Time: 24 h
CuONP_102	181.45 ± 18.12 235.90 ± 28.52 (98%) 4374.75 ± 486.84 (2%)	0.25 ± 0.03	203.01 ± 35.24 284.54 ± 55.11 (97%) 3481.33 ± 888.88 (3%)	0.30 ± 0.03

CuO-CIT NPs were well dispersed in EMEM medium+ supplements and the dispersions were stable for 24 hours at 28° C. Values in blue also appear in EMEM medium+ supplements with BSA and without NPs.

CuO-PEI NPs in EMEM (Lonza; Cat n° BE12-125F) + 1% L-Gln + 1% Pen/Strep + 1% non-essential amino acids + 10% FBS

Table 43 shows the characterization data of CuO-PEI NPs in the cell culture medium.

Table 43 - Particle size distribution of NPs dispersions in cell culture medium (at 100 µg/mL). Blue values refer to EMEM medium+ supplements with BSA and without NPs.

Nanoparticle	Z-aver and PSD (Mean dm in nm ± SEM) Time: 0 h	PdI Time: 0 h	Z-aver and PSD (Mean dm in nm ± SEM) Time: 24 h	PdI Time: 24 h
CuONP_104	335.82 ± 63.48 416.93 ± 77.54 (81%) 61.64 ± 30.63 (3%) 4379.78 ± 582.64 (16%)	0.4 ± 0.07	250.05 ± 82.36 430.48 ± 88.29 (86%) 52.78 ± 18.78 (4%) 2706.43 ± 1363.30 (10%)	0.55 ± 0.10

CuO-PEI NPs were well dispersed in EMEM medium+ supplements and the dispersions were stable for 24 hours at 28° C. Values in blue also appear in EMEM medium+ supplements with BSA and without NPs.

CuO-ASC NPs in EMEM (Lonza; Cat n° BE12-125F) + 1% L-Gln + 1% Pen/Strep + 1% non-essential amino acids + 10% FBS

Table 44 shows the characterization data of CuO-ASC NPs in the cell culture medium.

Table 44 - Particle size distribution of NPs dispersions in cell culture medium (at 100 µg/mL). Blue values refer to EMEM medium+ supplements with BSA and without NPs.

Nanoparticle	Z-aver and PSD (Mean dm in nm ± SEM) Time: 0 h	PdI Time: 0 h	Z-aver and PSD (Mean dm in nm ± SEM) Time: 24 h	PdI Time: 24 h
CuONP_105	159.43 ± 14.32 266.25 ± 36.80 (97%) 3878.83 ± 514.70 (3%)	0.41 ± 0.03	146.22 ± 27.01 208.22 ± 50.83 (99%) 4604.13 ± 140.34 (1%)	0.29 ± 0.02

CuO-ASC NPs were well dispersed in EMEM medium+ supplements and the dispersions were stable for 24 hours at 28° C. Values in blue also appear in EMEM medium+ supplements with BSA and without NPs.

Deviations from the Workplan

According to high dissolution rates observed for CuO NPs dispersed in media at acid pH, such as artifical lysosomial fluid (data published in Gosens et al., 2016), TEM-EDX analysis on tissues and organs to detect CuO NPs was not performed.

Performance of the partners

The Partners that have contributed to this task have been: UNIVE, VN, RIVM, CNR-ISTEC, INIA and UoP.
Besides the general delay from the work plan described above all partners have fulfilled their tasks.

Conclusions

The characterization of different pristine and modified SUN samples in several *in vitro* (i.e. MEM, DMEM, Leibovitz´s L-15 and EMEM) and environmental (artificial fresh and marine waters) media has been reported. Moreover, the intrinsic hazard of pristine and modified CuO NPs has been investigated by Cu quantification in tissues from short term inhalation and oral studies.

Annex

Table A1 - Composition (g/l) of the different media tested.

	PBS (Sigma Aldrich D8662)	MEM (Sigma Aldrich M2279)	DMEM (Gibco 41966)	AFW (OECD 1992)	AMW (ASTM D1141)
Inorganic salts	g/L	g/L	g/L	g/L	g/L
$CaCl_2 \cdot 2H_2O$	0.133	0.265	0.264	0.294	1.47
$Fe(NO_3)_3 \cdot 9H_2O$	-	-	0.0001	-	-
$MgSO_4$ (anhydrous)	-	0.098	-	-	-
$MgSO_4 \cdot 7H_2O$	-	-	0.2	0.123	-
$MgCl_2 \cdot 6H_2O$	0.1	-	-	-	10.8
KCl	0.2	0.4	0.4	0.006	0.7
KH_2PO_4	0.2	-	-	-	-
$NaHCO_3$	-	2.2	3.7	0.064	0.2
NaCl	8	6.8	6.4	-	23.5
Na_2HPO_4 (anhydrous)	1.15	-	-	-	-
NaH_2PO_4 (anhydrous)	-	0.122	-	-	-
$NaH_2PO_4 \cdot 2H_2O$	-	-	0.141	-	-
Na_2SO_4	-	-	-	-	4.0
$SrCl_2$ 6H2O	-	-	-	-	0.02
H_3BO_3	-	-	-	-	0.03
KBr	-	-	-	-	0.10
Na_2O_3Si $9H_2O$	-	-	-	-	0.02

Amino acids		g/l	g/L
Glycine		-	0.03
L-Arginine · HCl		0.126	0.084
L-Cystine · 2HCl		0.0313	0.063
L-Glutamine		0.292	0.58
L-Histidine · HCl · H20		0.042	0.042
L-Isoleucine		0.052	0.105
L-Leucine		0.052	0.105
L-Lysine · HCl		0.0725	0.146
L-Methionine		0.015	0.03
L-Phenylalanine		0.032	0.066
L-Serine		-	0.042
L-Threonine		0.048	0.095
L-Tryptophan		0.01	0.016
L-Tyrosine · 2Na · 2H20		0.0519	0.072
L-Valine		0.046	0.094

Vitamins		g/l	g/L
Choline chloride		0.001	0.004
D-Calcium pantothenate		-	0.004
Folic acid		0.001	0.004
myo-Inositol		0.002	0.0072
Niacinamide		0.001	0.004
D-Pantothenic acid • ½Ca		0.001	-
Pyridoxal • HCl		0.001	0.004
Riboflavin		0.0001	0.0004
Thiamine · HCl		0.001	0.004

Other		g/l	g/L
Glucose		1	4.5
Phenol red ·Na		0.011	0.015
Sodium Pyruvate		-	0.11

References

ASTM D1141-98 (Re-approved 2003) Standard Practice for the Preparation of Substitute Ocean Water.

Catalano F, Accomasso L, Alberto G, Gallina C, Raimondo S, Geuna S, Giachino C, Martra G. Factors Ruling the Uptake of Silica Nanoparticles by Mesenchymal Stem Cells: Agglomeration Versus Dispersions, Absence Versus Presence of Serum Proteins, Small 2015, 11, 2919–2928.

Cronholm P, Karlsson HL, Hedberg J, Lowe TA, Winnberg L, Elihn K, Odnevall Wallinder I, Möller L. Intracellular Uptake and Toxicity of Ag and CuO Nanoparticles: A Comparison Between Nanoparticles and their Corresponding Metal Ions, Small 9 (2013) 970-982.

Gosens I, et al., Organ burden and pulmonary toxicity of nanosized copper (II) oxide particles after short-term inhalation exposure. Nanotoxicology 2016, 2:1-12.

Hsiung C et al., Minimizing interferences in the quantitative multielement analysis of trace elements in biological fluids by inductively coupled plasma mass spectrometry, Clinical Chemistry 43 (1997), 2303-2311.

Karimi I, Hashemi B, Javidi M, Azadani SN. Studying effect of various stabilisers on sol electrophoretic deposition of titania, Surface Eng. 28 (2012) 737–742.

Ji ZX, Jin X, George S, Xia TA, Meng HA, Wang X, Suarez E, Zhang HY, Hoek EMV, Godwin H, Nel AE, Zink JI. Dispersion and Stability Optimization of TiO2 Nanoparticles in Cell Culture Media, Environ. Sci. Technol. 44 (2010) 7309–7314.

Karlsson HL, Cronholm P, Hedberg Y, Tornberg M, De Battice L, Svedhem S, Wallinder IO. Cell membrane damage and protein interaction induced by copper containing nanoparticles-Importance of the metal release process, Toxicology 313 (2013) 59–69.

Liu X, Chen L. Aggregation and interactions of chemical mechanical planarization nanoparticles with model biological membranes: role of phosphate adsorption, Environ. Sci.: Nano 3 (2016) 146-156.

McFarlane NL, Wagner NJ, Kaler EW, Lynch ML, Poly(ethylene oxide) (PEO) and Poly(vinyl pyrolidone) (PVP) Induce Different Changes in the Colloid Stability of Nanoparticles, Langmuir 26 (2010) 13823–13830.

Midander K, Cronholm P, Karlsson HL, Elihn K, Möller L, Leygraf C, Odnevall Wallinder I. Surface Characteristics, Copper Release, and Toxicity of Nano- and Micrometer-Sized Copper and Copper(II) Oxide Particles: A Cross-Disciplinary Study, Small 5 (2009) 389-399.

Mudunkotuwa, IA. Grassian VH. Biological and environmental media control oxide nanoparticle surface composition: the roles of biological components (proteins and amino acids), inorganic oxyanions and humic acid. Environ. Sci: Nano 2 (2015):429-439.

Nomura CS et al., Bovine liver sample preparation and micro-homogeneity study for Cu and Zn determination by solid sampling electrothermal atomic absorption spectrometry, Spectrochimica Acta Part B 60 (2005), 673– 680.

OECD (1992) Guidelines for Testing of Chemicals No. 203. Fish, Acute Toxicity Test (Annex 2 Composition of the recommended reconstituted water). OECD, Paris.

Rodrìguez LC et al., Principles of analytical calibration/quantification for the separation sciences, Journal of Chromatography A 1158 (2007), 33–46.

Semisch A, Ohle J, Witt B, Hartwig A. Cytotoxicity and genotoxicity of nano – and microparticulate copper oxide: role of solubility and intracellular bioavailability, Particle and Fibre Toxicology 11 (2014) 10.

Table 23 – Copper concentration from pristine CuO NPs. Ø represents empty sample and § represents mistake over digestion process.

Sample N°	Organs			Sample N°	Liver		Lung		Kidney		Spleen		MLN		Thymus		Testis		Cortex		Autopsy day	Bodyweight (mg/Kg)
N°	Value (mg/Kg)	RSD %																				
	mg dry weight																					
			CuO	5	756.72	0.5%	119.12	0.4%	77.32	0.4%	7.39	1.0%	20.78	1.0%	10.91	1.0%	11.29	0.7%	9.14	1.1%	5	512
					235.35		194.69		133.11		84.54		24.62		83.56		220.91		43.01			
				6	1001.53	0.3%	14.95	1.2%	43.15	0.5%	17.36	0.7%	14.93	0.9%	6.61	1.2%	11.99	0.8%	10.04	1.1%		
					249.66		224.23		113.48		68.92		13.47		45.74		222.57		39.45			
				7	298.95	0.9%	6.63	1.0%	49.16	0.6%	6.49	0.9%	30.73	0.9%	4.70	0.8%	10.50	0.4%	9.58	1.2%		
					196.44		199.39		144.96		71.9		20.2		88.92		252.4		35.41			
				8	1596.99	0.8%	140.02	0.6%	135.99	0.4%	8.66	0.6%	38.61	1.4%	19.33	0.8%	12.57	1.0%	10.48	0.9%		
					237.13		179.65		119.6		41.71		11.85		32.88		199.62		43.15			
				1	13.53	0.7%	5.77	0.8%	36.93	1.4%	6.67	1.8%	4.29	2.5%	4.15	1.3%	10.46	0.6%	8.71	0.6%	6	vehicle control
					209.35		145.27		292.39		37.47		12.8		58.33		199.85		119.59			
				2	12.79	0.6%	5.68	0.7%	37.82	0.5%	5.69	2.0%	4.76	1.4%	3.91	1.0%	10.37	0.6%	8.51	0.9%		
					219.56		116.07		245.16		35.56		11.62		62.77		181.38		113.99			
				3	13.53	1.5%	7.30	0.3%	50.48	0.7%	5.94	0.7%	5.15	2.2%	3.89	0.9%	10.92	1.0%	8.53	0.9%		
					200.14		134.12		260.36		37.62		15.04		57.22		177.89		117.63			
				4	13.81	0.5%	5.03	0.7%	39.75	0.7%	6.08	1.0%	5.68	2.9%	3.53	2.0%	10.78	0.9%	8.55	0.8%		
					247.23		146.01		259.88		33.88		12.7		62.01		183.35		114.53			
				25	36.13	0.4%	5.79	0.6%	52.50	0.9%	5.21	0.8%	Ø		4.88	1.3%	10.48	0.8%	9.05	0.4%		32
					243.22		146.33		230.66		54.88				76.58		200.11		110.13			
				26	61.12	1.0%	6.38	0.4%	48.61	0.5%	5.86	0.8%	6.96	2.8%	4.09	0.6%	10.56	0.1%	8.89	0.6%		
					200.48		136.05		211.86		48.57		13.65		58.17		189.79		111.66			
				27	24.16	0.6%	5.38	0.4%	72.78	0.6%	5.68	3.4%	10.12	2.5%	15.18	0.8%	10.80	1.1%	8.31	0.3%		
					216.23		155.22		272.21		40.09		7.26		47.3		186.67		118.98			
				28	45.83	0.4%	4.51	1.0%	76.11	0.5%	5.62	1.1%	6.51	1.1%	5.49	0.3%	10.73	1.1%	8.04	0.8%		
					196.35		170.88		302.22		45.71		17.73		71.14		212.41		114.3			
				29	71.31	0.7%	5.43	0.4%	64.34	0.9%	5.66	0.6%	9.79	1.3%	5.34	0.7%	11.13	0.7%	Ø		7	64
					261.21		187.1		270.87		40.09		6.11		58.41		188.25					
				30	77.73	0.5%	Ø		§		6.83	1.2%	10.27	2.1%	11.29	0.6%	10.73	0.5%	Ø			
					207.49						37.23		3.1		50.6		191.79					
				31	13.89	0.5%	7.04	0.4%	74.88	0.5%	6.65	0.5%	3.79	2.8%	6.08	0.3%	12.44	0.6%	13.49	0.1%	26	Vehicle control
					222.15		152.9		269.63		45.01		16.53		47.23		200.31		102.73			
				32	13.73	0.8%	6.78	0.4%	58.18	0.8%	5.44	1.1%	6.87	0.9%	5.19	1.0%	12.39	1.2%	9.83	0.3%		
					248.16		169.69		283.93		45.71		20.2		56.69		203.15		108.4			
				33	13.25	0.4%	6.78	0.6%	56.07	0.6%	5.44	1.3%	2.57	3.8%	4.00	1.8%	11.62	0.5%	7.10	0.7%		
					235.66		147.66		307.66		42.18		5.84		58.26		190.93		113.34			
				34	13.75	0.8%	6.61	0.8%	56.95	1.1%	5.58	1.4%	3.07	2.3%	4.27	1.0%	13.11	0.7%	9.94	0.5%		
					223.54		147.48		274.4		36.64		15.57		41.88		186.74		111.63			
				55	13.43	0.8%	8.33	0.4%	55.32	0.8%	6.68	3.1%	2.83	2.4%	4.26	0.6%	10.98	0.5%	8.46	0.9%		
					237.85		152.99		139.59		37.12		26.29		63.64		220.41		116.85			

Table 24 - Copper concentration from $CuCO_3$.

Sample N°	Organs			Sample N°	Liver		Lung		Kidney		Spleen		MLN		Thymus		Testis		Cortex		Autopsy day	Bodyweight (mg/Kg)
N°	Value (mg/Kg)	RSD %																				
	mg dry weight																					
			$CuCO_3$	57	13.55	0.9%	7.35	0.5%	37.48	1.1%	4.93	0.5%	6.63	1.2%	3.84	3.1%	11.56	0.9%	8.75	0.6%	5	Vehicle control
					203.29		181.68		164.99		99.96		17.12		68.25		220.51		41.47			
				58	12.23	2.1%	7.81	1.6%	27.46	0.5%	4.57	0.9%	7.22	0.6%	2.88	0.6%	11.09	0.5%	8.57	1.3%		
					234.8		207.15		142.45		79.45		11.25		96.56		225.44		31.47			
				59	12.89	0.5%	7.88	1.1%	26.34	0.4%	5.04	1.2%	5.01	1.0%	3.53	3.5%	11.71	1.2%	8.93	1.7%		
					226.99		164.47		135.3		59.9		32.01		94.54		224.2		33.32			
				60	12.85	0.8%	7.14	0.9%	24.71	0.7%	4.77	0.7%	5.21	0.2%	3.96	1.4%	11.12	1.0%	8.68	1.1%		
					233.6		176.25		151.32		92.12		29.69		66.68		198.47		41.96			
				65	366.61	0.6%	7.86	1.0%	49.99	0.6%	6.12	0.5%	8.56	0.8%	5.75	0.4%	11.94	1.2%	9.97	0.9%		64
					217.56		158.32		104.3		86.75		17.16		104.3		215.83		25.05			
				66	499.52	0.2%	8.05	0.5%	44.79	0.2%	5.55	1.1%	6.46	1.2%	7.22	1.2%	11.83	0.9%	9.91	1.2%		
					215.4		196.56		53.32		78.6		17.28		53.32		197.27		39.4			
				67	460.28	0.7%	13.83	0.3%	131.63	0.7%	6.37	0.4%	7.59	1.0%	6.05	0.6%	12.21	0.5%	9.31	0.7%		
					247.81		265.84		111.05		111.39		17.82		111.05		243.63		53.22			
				68	475.67	0.5%	6.88	0.7%	69.68	0.7%	5.11	0.6%	7.29	1.8%	6.33	1.0%	11.75	0.9%	9.15	0.9%		
					211.02		206.72		87.98		83.65		6.78		87.98		202.68		36.47			
				61	1470.29	0.6%	946.13	0.5%	563.45	0.4%	18.57	0.5%	40.08	0.8%	34.08	1.1%	15.13	0.8%	9.82	0.4%		128
					213.29		146.98		140.66		48.09		19.64		30.64		193.03		42.4			
				62	1034.32	0.7%	595.24	0.6%	1006.89	0.7%	164.14	0.5%	56.09	0.6%	64.56	0.8%	20.63	0.4%	11.20	0.7%		
					216.58		218.17		136.62		49.49		17.7		16.42		202.55		38.51			
				63	1161.22	0.8%	43.98	0.4%	1273.68	0.8%	70.57	0.7%	32.64	0.6%	46.68	1.0%	17.21	0.7%	12.39	1.5%		
					233.52		191.32		34.86		63.65		17.56		34.86		223.44		36.18			
				64	1531.13	0.8%	143.79	0.7%	481.27	0.7%	14.99	1.0%	36.70	0.9%	35.68	0.6%	14.47	0.7%	9.68	0.6%		
					230.49		174.78		26.28		34.62		17.23		26.28		205.11		33.46			
				91	1231.44	0.6%	10.86	0.3%	314.17	0.2%	12.80	1.4%	92.87	0.7%	12.87	1.4%	12.95	0.6%	9.62	1.0%		
					237		152.13		116.03		28.96		22.28		29.94		203.59		45.74			
				92	1182.06	0.7%	117.62	0.3%	573.12	0.5%	13.88	1.0%	35.44	0.6%	19.70	0.4%	10.71	0.5%	10.52	1.0%		
					198.56		170.05		128.02		57.58		21.82		38.74		206.54		37.82			
				89	1975.06	0.8%	182.88	0.9%	1233.53	0.6%	60.08	0.8%	67.34	1.2%	12.59	0.8%	16.78	1.3%	11.48	1.1%	6	
					201.35		180.16		132.48		46.48		10.65		17.39		232.53		27.04			
				90	1603.56	0.7%	28.02	0.5%	1037.43	0.6%	56.79	0.9%	22.56	0.5%	7.62	0.9%	15.83	0.5%	10.18	1.2%		
					214.27		200.92		169.03		67.66		18.81		26.13		232.96		45.02			
				85	12.38	0.6%	7.31	0.9%	61.33	0.5%	4.95	0.5%	4.62	0.7%	3.32	0.3%	10.86	0.9%	8.94	1.4%	26	Vehicle control
					210.32		242.33		146.46		124.32		25.15		73.15		239.24		38.16			
				86	14.24	1.6%	6.52	0.8%	24.70	0.6%	4.59	0.8%	10.28	1.1%	2.82	1.3%	11.11	0.4%	9.40	0.7%		
					197.32		234.93		166.75		90		10.03		115.76		240		35.66			
				87	12.27	0.6%	6.94	0.9%	27.69	0.6%	4.85	0.9%	4.20	2.9%	2.53	0.9%	10.57	0.7%	8.61	1.3%		
					191.91		239.77		198.5		85.82		23.16		116.37		262.42		36.11			
				88	12.05	0.9%	7.14	0.6%	30.40	0.5%	5.07	1.0%	4.06	1.1%	2.78	1.3%	11.05	0.7%	9.64	0.9%		
					204.8		195.43		172.7		69.08		26.62		80.12		247.83		34.4			
				93	20.92	1.5%	6.47	0.3%	32.27	0.4%	4.60	1.2%	7.07	2.3%	3.28	0.3%	12.21	0.9%	9.23	0.5%		64
					207.09		219.23		212.1		89.76		7.86		84.66		245.91		38.64			
				94	29.49	0.7%	7.06	0.4%	22.92	0.6%	4.85	0.9%	4.86	0.9%	3.04	1.6%	12.48	0.5%	8.58	0.7%		
					215.63		249.04		182.72		70.14		14.42		99.95		252.26		29.63			
				95	41.61	0.6%	7.84	0.8%	31.09	0.6%	5.26	1.3%	7.80	0.9%	3.86	0.9%	14.33	1.4%	19.54	0.9%		
					173.94		190.02		145.69		95.95		20.93		96.61		224.39		37.07			
				96	23.06	0.5%	7.54	0.5%	26.74	1.1%	4.78	0.8%	3.82	2.4%	2.95	1.0%	13.46	1.3%	2.46	1.3%		
					213.42		227.16		173.09		105.58		23.3		109.19		261.65		40.91			

As far as the media without amino acids and proteins (MilliQ, PBS, AFW and AMW), it was observed that the highest values were found for CuO-CIT and CuO-PEI dispersions. This confirms that the particle dissolution rate depends on the CuO NPs characteristics as well as on the chemical composition of the medium surrounding NPs, unless the features of the medium not prevail over the complete system (Cronholm et al., 2013). Furthermore, in support to this, a size dependent solubility is shown in the samples dispersed in MilliQ and PBS. At low aggregation rate corresponds a high solubility (CuO-CIT and CuO-PEI). Otherwise, the samples resulted more aggregated (CuO-pristine, CuO-PVP and CuO-ASC) showed very low values of $Cu_{dissolved}/Cu_{total}$ weight ratio (%).

Conclusions

Four different non-hazardous modifying agents, sodium citrate (CIT), sodium ascorbate (ASC), branched polyethylenimine (PEI) and polyvinylpyrrolidone (PVP), were added to CuO NP suspensions for promoting the *in situ* coating of particles within a Safety by Design approach. The good agreement among NPs size, ζ-pot, sedimentation velocity and dissolution results confirmed that the combined techniques represent an effective tool for the colloidal stability evaluation. Biological components (amino acids and proteins) and inorganic salts (oxyanions and divalent cations) resulted to be key determinant factors driving colloidal stability of both pristine and modified CuO NPs. The comprehensive colloidal characterization performed, following the evolution of pristine and modified CuO NP properties at increasing medium complexity (from MilliQ water to biological and environmental fluids), will contribute to better describe the interactions between NPs and the components of the surrounding medium, including amino acids, proteins, divalent cations and phosphates and would greatly support the interpretation of toxicological and ecotoxicological outcomes.

2 Cu quantification in tissues and organs from *in vivo* studies

Quantification of Cu in tissues and organs from Short Term Inhalation Studies (STIS) 1 and 2 as well as from Short Term Oral Study (STOS), all of which carried out by RIVM, has been performed. Materials, methods and results for each study are reported here below.

STIS 1 - pristine CuO NPs

Organs and tissues collected from rats exposed to short term inhalation study with pristine CuO NPs performed by RIVM were received by VenetoNanotech (VN) on 24/07/2014, 22/10/2014, and 18/11/2014, as listed in Table 4. Accordingly, the quantification of Cu in tissues and organs from this STIS 1 has been carried out by VN.

Table 4 - List of tissue and organ amples (continues).

Delivery date	Amount	Sample	Average weight ± standard deviation – analysed samples (mg)	Notes
24/07/2014	32	Lung from rats exposed to STIS	352 ± 84	Lung samples were freeze-dried after dissection, shipped and stored at room temperature until analysis.
	6	Empty tube (control)	/	Tubes were filled with ultrapure water, stored on dry ice, freeze dried, shipped and stored following the same method applyed for organ samples.
22/10/2014	32	Blood from rats exposed to STIS	4518 ± 730	Blood samples were collected in K3-EDTA tubes, frozen, shipped and stored at -20 °C until analysis. The tube corresponding to rat#12 was empty.
	6	Frozen water (control)	3850 ± 1027	K3-EDTA tubes containing frozen water, shipped and stored as blood samples.
	32	Bone marrow rats exposed to STIS	5496 ± 679	Bone marrow samples were collected in tubes, frozen, shipped and stored at -20 °C until analysis.
	6	Frozen water (control)	5247 ± 685	Tubes containing frozen water, shipped and stored as bone marrow samples.

Table 4 - List of tissue and organ amples.

Delivery date	Amount	Sample	Average weight ± standard deviation – analysed samples (mg)	Notes
18/11/2014	16	Brain from rat exposed to STIS	222 ± 17	
	16	Liver from rat exposed to STIS	200 ± 5*	
	16	Spleen from rat exposed to STIS	167 ± 25	
	16	Heart from rat exposed to STIS	257 ± 26	All the organs were freeze-dried and crumbled after dissection, shipped and stored at room temperature until analysis. * Weight of the analysed aliquots
	16	Kidney from rat exposed to STIS	590 ± 185	
	16	Testis from rat exposed to STIS	/	
	16	Epididymis from rat exposed to STIS	/	
	6	empty tube (control)	/	Tubes were filled with ultrapure water, stored on dry ice, freeze dried, shipped and stored following the same method applyed for organ samples.
	3	empty cryovials (control)	/	

Materials and methods

Sample preparation

Lungs

Each freeze-dried lung was put into a polyethylene sterile bag covered with a fluffy folded paper. Each sample was subsequently crushed with a ceramic pestle to obtain a powder, needed for the digestion process. The empty tubes (controls) were filled with 5 mL of ultrapure water and digested as the lung samples.

Blood and bone marrow samples

The samples have been allowed to thaw out at room temperature and transferred in the digestion vessels.
In agreement with RIVM, the analysis was performed only for the animals belonging to the control and to the highest doses tested.

Other organs

As testis and epididymis samples were not completely freeze-dried, in agreement with RIVM, they were not analysed as well as the corresponding controls (3 empty cryovials).
Staring from an amount of 4 g, liver samples were grounded, homogenized and an aliquot of about 200 mg was used for the microwave acid digestion. All the other samples (brain, spleen, heart and kidney) were suitable to be entirely analyzed, so the crumbled organs were transferred in the digestion vessels. The empty tubes (controls) were filled with 5 mL of ultrapure water and digested as the organ samples. Likewise to blood and bone marrow samples, only the organs collected from the animals belonging to the control and the highest concentrations were analysed.

Acid digestion

The acid mixture used for samples mineralization was composed by HNO_3 (distilled Selected Assured Acid 69%, Romil), H_2O_2 (Super Purity Reagent 30%, Romil) and H_2O (ultrapure water 18.3 $M\Omega \cdot cm^{-1}$, Human), in the 2:1:3 ratio. After the addition of nitric acid, the samples were left under a fume hood over two hours, then the hydrogen peroxide was added and the vessels stood opened under the fume hood overnight. This pre-digestion step allowed the release of CO_2, avoiding damages caused by an excessive increase of the internal pressure in the digestion vessels during the heating program.
After the pre-digestion step, ultrapure water was added and the vessels were placed in the microwave system (MARS V, CEM), using the heating program (Nomura et al., 2005) reported in Table 55. Aftewards, the samples were allowed to cool down for 30 minutes at room temperature and in a cold room (temp. +4°C) for one hour. The obtained solutions were transferred in polyethylene tubes and diluted to 50 mL with ultrapure water.

Table 5 - Heating program for acid digestion of the lungs samples.

STAGE	RAMP TIME (min)	TEMPERATURE (°C)	HOLD TIME (min)
1	5	140	1
2	8	180	2
3	4	200	10

ICP-MS analysis

The sample solutions were properly diluted and analyzed by inductively coupled plasma mass spectrometry equipped with dynamic reaction cell (DRC-ICP-MS NexION 300D, Perkin Elmer) and ammonia was used as reagent gas.
For the quantification of copper, isotope ^{65}Cu was selected because of the less polyatomic interferences (e.g. $^{40}Ar^{23}Na$) than isotope ^{63}Cu (Hsiung et al., 1997). Samples were analyzed by external calibration method using a multi-point curve (blank and 6 points from 0.5 to 25 $\mu g\ L^{-1}$), except for the bone marrows, which were analysed by standard addition method to avoid matrix interferences (Rodrìguez et al., 2007).
Rhodium at 10 $ug \cdot L^{-1}$ was added as internal standard element.

QA/QC

Potential contamination from the VN laboratory was controlled by adding at least one reagent blank during every digestion process.
To control the overall contamination, including the freeze-drying process, shipping and storage steps, procedural blanks constituted by the control samples sent togheter with the organ and tissue samples (empty tubes/cryovials and tubes/cryovials filled with frozen water) were analysed.

The limit of detection (LOD) and the limit of quantification (LOQ) were calculated for each sample set (i.e. lungs, blood, bone marrow, all the other organs) as the average of blanks + 3 standard deviation (SD) and as the average of blanks + 10 SD, respectively.
In order to verify the accuracy and repeatability of the method, 20 aliquots (prepared in 12 different days) of the standard reference material (SRM) NIST 1577c (bovine liver) were analyzed.

Results

Accuracy
The mean Cu concentration detected in the SRM is 261.2 ± 10.1 $mg \cdot kg^{-1}$, in agreement with the reference value (275.2 ± 4.6 $mg \cdot kg^{-1}$).

Recovery
With respect to the certified value, the recovery of Cu ranged from 90 % to 104 %.

Repeatability
Repeatability was calculated as relative standard deviation of the 20 different SRM aliquots and it is 4 %.

LOD/LOQ
Since some of the blanks analyzed had a signal below or comparable to the instrumental calibration blank, their values were set as half of the first point of the calibration curve.
Average blank values, LOD and LOQ were calculated by considering both the reagent blanks and the control blanks.

Lung
The Cu concentration in blanks was 2 ± 3 $\mu g \cdot L^{-1}$ (average value ± SD), the LOD was 10 $\mu g \cdot L^{-1}$ and the LOQ was 30 $\mu g \cdot L^{-1}$.

Blood
The Cu concentration in blanks was 2 ± 1 $\mu g \cdot L^{-1}$ (average value ± SD), the LOD was 5 $\mu g \cdot L^{-1}$ and LOQ was 12 $\mu g \cdot L^{-1}$.

Bone marrow
As the Cu concentration in bone marrow blanks was always comparable with the calibration blank value, it was calculated as described above and it resulted 2.36 ± 0.02 $\mu g \cdot L^{-1}$ (average value ± SD); the LOD was 2.43 $\mu g \cdot L^{-1}$ and LOQ was 2.58 $\mu g \cdot L^{-1}$.

Other organs (brain, liver, heart, spleen and kidney)
For other organs the Cu concentration in blanks was 1 ± 1 $\mu g \cdot L^{-1}$ (average value ± SD), the LOD was 5 $\mu g \cdot L^{-1}$ and LOQ was 13 $\mu g \cdot L^{-1}$.

Copper concentration in tissues and organs
Copper concentration in tissues and organs from rats exposed to STIS, expressed on a dry weight basis, are shown from Table 6 to Table 13. Average values and standard deviations associated to three ICP-MS readings are reported. Since the mean of the blanks affected the samples concentration less than 10 %, the results were not corrected for the blank values.

Table 6 – Copper concentration in lung samples.

LUNG				
Group	Rat #	Sample ID	Cu ($mg \cdot kg^{-1}$)	SD ($mg \cdot kg^{-1}$)
1C	11	Lung-11	9.4	0.3
1C	12	Lung-12	8.81	0.01
1C	13	Lung-13	9.23	0.09
1C	14	Lung-14	8.61	0.04
1D	15	Lung-15	8.15	0.03
1D	16	Lung-16	8.50	0.07
1D	17	Lung-17	8.50	0.06
1D	18	Lung-18	8.91	0.04
2C	29	Lung-29	10.97	0.09
2C	30	Lung-30	10.17	0.04
2C	31	Lung-31	10.84	0.08
2C	32	Lung-32	11.03	0.05
2D	33	Lung-33	8.25	0.05
2D	34	Lung-34	7.11	0.04
2D	35	Lung-35	8.18	0.07
2D	36	Lung-36	9.98	0.05
4C	57	Lung-57	29.2	0.1
4C	58	Lung-58	22.6	0.1
4C	59	Lung-59	27.2	1.0
4C	60	Lung-60	30.9	0.3
4D	61	Lung-61	7.445	0.005
4D	62	Lung-62	9.3	0.1
4D	63	Lung-63	8.24	0.04
4D	64	Lung-64	8.07	0.05
6C	85	Lung-85	51.4	0.6
6C	86	Lung-86	53.6	0.4
6C	87	Lung-87	57.3	0.5
6C	88	Lung-88	48.3	0.1
6D	89	Lung-89	8.55	0.07
6D	90	Lung-90	8.46	0.06
6D	91	Lung-91	8.4	0.1
6D§	92§	Lung-92§	7.45	0.03

§ The value could not be completely reliable because of a mistake over digestion process.

Table 7 – Copper concentration in blood samples.

BLOOD				
Group	Rat #	Sample ID	Cu ($mg \cdot kg^{-1}$)	SD ($mg \cdot kg^{-1}$)
1C	11	Blood-11	0.793	0.004
1C	13	Blood-13	0.78	0.02
1C	14	Blood-14	0.693	0.004
1D	15	Blood-15	0.828	0.002
1D	16	Blood-16	0.874	0.004
1D	17	Blood-17	0.89	0.02
1D	18	Blood-18	0.79	0.01
6C	85	Blood-85	0.89	0.01
6C	86	Blood-86	0.886	0.007
6C	87	Blood-87	0.797	0.005
6C	88	Blood-88	0.87	0.01
6D	89	Blood-89	0.913	0.003
6D	90	Blood-90	0.920	0.002
6D	91	Blood-91	0.86	0.01
6D	92	Blood-92	0.782	0.005

Table 8 – Copper concentration in bone marrow samples. B.D.L.=below detection limit

BONE MARROW				
Group	Rat #	Sample ID	Cu ($mg \cdot kg^{-1}$)	SD ($mg \cdot kg^{-1}$)
1C	11	Bone marrow-11	0.029	0.001
1C	12	Bone marrow-12	0.052	0.001
1C	13	Bone marrow-13	0.037	0.003
1C	14	Bone marrow-14	0.0433	0.0002
1D	15	Bone marrow-15	0.0396	0.0004
1D	16	Bone marrow-16	0.039	0.001
1D	17	Bone marrow-17	0.053	0.001
1D	18	Bone marrow-18	0.036	0.003
6C	85	Bone marrow-85	0.041	0.007
6C	86	Bone marrow-86	B.D.L.	B.D.L.
6C	87	Bone marrow-87	0.033	0.001
6C§	88§	Bone marrow-88§	0.023§	0.001§
6D	89	Bone marrow-89	B.D.L.	B.D.L.
6D	90	Bone marrow-90	0.031	0.002
6D	91	Bone marrow-91	0.040	0.002
6D	92	Bone marrow-92	0.033	0.001

§ Data below the limit of quantitation.

Table 9 – Copper concentration in brain samples.

BRAIN				
Group	Rat #	Sample ID	Cu ($mg \cdot kg^{-1}$)	SD ($mg \cdot kg^{-1}$)
1C	11	Brain-11	9.3	0.1
1C	12	Brain-12	26.7	0.5
1C	13	Brain-13	9.8	0.2
1C	14	Brain-14	9.6	0.2
1D	15	Brain-15	10.58	0.02
1D	16	Brain-16	10.31	0.09
1D	17	Brain-17	9.7	0.3
1D	18	Brain-18	10.8	0.2
6C	85	Brain-85	10.17	0.06
6C	86	Brain-86	9.2	0.3
6C	87	Brain-87	8.4	0.1
6C	88	Brain-88	9.8	0.1
6D	89	Brain-89	11.25	0.09
6D	90	Brain-90	10.20	0.08
6D	91	Brain-91	9.5	0.2
6D	92	Brain-92	9.95	0.01

Table 10 – Copper concentration in liver samples.

LIVER				
Group	Rat #	Sample ID	Cu ($mg \cdot kg^{-1}$)	SD ($mg \cdot kg^{-1}$)
1C	11	Liver-11	12.7	0.5
1C	12	Liver-12	12.9	0.3
1C	13	Liver-13	13.9	0.2
1C	14	Liver-14	12.4	0.5
1D	15	Liver-15	12.9	0.5
1D	16	Liver-16	12.3	0.4
1D	17	Liver-17	13.1	0.2
1D	18	Liver-18	13.1	0.3
6C	85	Liver-85	12.5	0.2
6C	86	Liver-86	12.6	0.4
6C	87	Liver-87	12.9	0.2
6C	88	Liver-88	13.7	0.5
6D	89	Liver-89	11.1	0.2
6D	90	Liver-90	10.8	0.5
6D	91	Liver-91	12.0	0.4
6D	92	Liver-92	11.2	0.2

Table 11 – Copper concentration in heart samples.

HEART				
Group	Rat #	Sample ID	Cu ($mg \cdot kg^{-1}$)	SD ($mg \cdot kg^{-1}$)
1C	11	Heart-11	21.9	0.2
1C	12	Heart-12	20.0	0.1
1C	13	Heart-13	22.5	0.2
1C	14	Heart-14	21.5	0.3
1D	15	Heart-15	22.3	0.1
1D	16	Heart-16	21.2	0.2
1D	17	Heart-17	20.0	0.1
1D	18	Heart-18	20.0	0.1
6C	85	Heart-85	21.3	0.4
6C	86	Heart-86	21.6	0.1
6C	87	Heart-87	21.0	0.6
6C	88	Heart-88	21.6	0.5
6D	89	Heart-89	20.4	0.1
6D	90	Heart-90	19.8	0.3
6D	91	Heart-91	21.7	0.3
6D	92	Heart-92	20.16	0.03

Table 12 – Copper concentration in spleen samples.

SPLEEN				
Group	Rat #	Sample ID	Cu ($mg \cdot kg^{-1}$)	SD ($mg \cdot kg^{-1}$)
1C	11	Spleen-11	4.7	0.2
1C§	12§	Spleen-12§	5.0§	0.2§
1C	13	Spleen-13	4.8	0.2
1C	14	Spleen-14	4.7	0.1
1D	15	Spleen-15	4.7	0.4
1D	16	Spleen-16	5.4	0.1
1D	17	Spleen-17	4.9	0.2
1D	18	Spleen-18	5.09	0.08
6C	85	Spleen-85	4.79	0.07
6C	86	Spleen-86	5.33	0.06
6C	87	Spleen-87	5.1	0.1
6C	88	Spleen-88	5.1	0.2
6D	89	Spleen-89	5.00	0.09
6D	90	Spleen-90	5.5	0.1
6D	91	Spleen-91	4.73	0.07
6D	92	Spleen-92	5.11	0.01

§Data below the limit of quantitation

Table 13 – Copper concentration in kidney samples.

KIDNEY				
Group	Rat #	Sample ID	Cu ($mg \cdot kg^{-1}$)	SD ($mg \cdot kg^{-1}$)
1C	11	Kidney-11	65.6	0.8
1C	12	Kidney-12	62.6	0.1
1C	13	Kidney-13	38.1	0.3
1C	14	Kidney-14	87.7	1.4
1D	15	Kidney-15	66.3	0.8
1D	16	Kidney-16	96.8	2.1
1D	17	Kidney-17	89.9	1.6
1D	18	Kidney-18	36.6	0.9
6C	85	Kidney-85	25.5	0.3
6C	86	Kidney-86	96	1
6C	87	Kidney-87	50.5	0.3
6C	88	Kidney-88	109	1
6D	89	Kidney-89	102.1	0.4
6D	90	Kidney-90	56.5	0.5
6D	91	Kidney-91	109	3
6D	92	Kidney-92	89	2

STIS 2 - modified CuO NPs

Within the WP7 “Safe production, handling and disposal”, focusing on the development of a Safe by Design ($S_{by}D$) approach to promote sustainable nanomanufacturing, the surface of pristine CuO nanoparticles has been modified with four different capping agents to obtain CuO nanoparticles with: positively charged polyethylenimine (PEI), negatively charged sodium citrate (CIT) and sodium ascorbate (ASC) as well as neutral polyvynilpyrrolinde (PVP). Among all the modified samples, this second short term inhalation study (STIS), performed by RIVM within WP6, aimed at evaluating if the pristine CuO nanoparticles toxicity changed comparing to PEI and ASC CuO nanoparticles toxicity. Organs and tissues collected from rats exposed to STIS 2 were received by UNIVE on 18/11/2015 and 09/12/2015, as listed in Table 14. The quantification of Cu in tissues and organs from this STIS has been carried out by UNIVE. All the organs describe in Table 14 were freeze-dried and crumbled after dissection, shipped at room temperature and stored in the frige (4 °C) until analysis. The average wheigh of each sample was 250 mg. Concentration range of the inhalation test were 0, 1.7, 15 mg/m^3 for CuO PEI and 0, 2.2, 20 mg/m^3 for CuO ASC, respectively.

Table 14 – List of tissues and organs samples from STIS with modified CuO

Autopsy day	Amount	Analysed Sample
18/11/2015	20	Liver from rat exposed to different concentration of CuO PEI/ASC
	20	Brain from rat exposed to different concentration of CuO PEI/ASC
	20	Kidneys from rat exposed to different concentration of CuO PEI/ASC
	20	Lung from rat exposed to different concentration of CuO PEI/ASC
	20	Spleen from rat exposed to different concentration of CuO PEI/ASC
	20	Heart from rat exposed to different concentration of CuO PEI/ASC
9/12/2015	20	Liver from rat exposed to different concentration of CuO PEI/ASC
	20	Brain from rat exposed to different concentration of CuO PEI/ASC
	20	Kidneys from rat exposed to different concentration of CuO PEI/ASC
	20	Lung from rat exposed to different concentration of CuO PEI/ASC
	20	Spleen from rat exposed to different concentration of CuO PEI/ASC
	20	Heart from rat exposed to different concentration of CuO PEI/ASC

Materials and methods

Acid digestion

The acid mixture used for samples mineralization included HNO_3 (trace select ultra 69%, Sigma-Aldrich <0.5µg/Kg), H_2O_2 (trace select ultra 30%, Sigma-Aldrich <0.05µg/Kg), in a 2:1 ratio. The microwave system ETHOS 1600, Milestone was used to digest the samples, following the procedure reported in Table 5Table 15. Afterwards, the samples were allowed to cool down for 30 minutes at room temperature. The obtained solutions were transferred in PTFE tubes and diluted to 25 mL with MilliQ water.

Table 15 - Heating program for acid digestion of the samples.

STAGE	RAMP TIME (min)	POWER (Watt)
1	1	250
2	1	0
3	5	250
4	3	400
5	3	600

ICP-MS analysis

An aliquot of each sample solution was properly diluted and analyzed by inductively coupled plasma mass spectrometry equipped with single channel Universal Cell (sp-ICP-MS NexION 350XXD, Perkin Elmer).
For the quantification of Copper, isotope ^{65}Cu was selected because of the less polyatomic interferences (e.g. $^{40}Ar^{23}Na$) than isotope ^{63}Cu. Moreover, to decrease interferences Kinetic energy discrimination (KED) was employed, using He as collision gas. Samples were quantified by external calibration method using a multi-point curve (blank and 10 points over the concentration range from 10 µg L^{-1} to 300 µg L^{-1}). Yttrium at 5 µg·L^{-1} was used as internal standard.

QA/QC

Potential contamination from the laboratory was controlled by adding at least one reagent blank during each digestion session.
The limit of detection (LOD) and the limit of quantification (LOQ) were calculated for each sample set as the average of blanks + 3 standard deviation (SD) and as the average of blanks + 10 SD, respectively.
In order to verify the accuracy and repeatability of the method, 6 aliquots of the standard reference material (SRM) NIST 1577c (bovine liver) were analysed every 10 samples.

Results

Accuracy

The average Cu concentration detected in the SRM was 277 ± 5 mg·kg^{-1}, in satisfactory agreement with the reference value (267 ± 6 mg·kg^{-1}).

Recovery

With respect to the certified value, the recovery of Cu ranged from 90 to 101%.

BEC

BEC is the background concentration signal providing the actual magnitude of noise. The detected BEC value was 0.033 µg·L^{-1}.

LOD/LOQ

Average blank values, LOD and LOQ were calculated by considering both the reagent and the control blanks. Detected LOD and LOQ value were, respectively, 153 ng·L^{-1} and 461 ng·L^{-1}.

Copper concentration in analysed organs

Copper concentration in tissues and organs from rats exposed to STIS, expressed on a dry weight basis, are shown from Table 16 to Table 21. Average values and standard deviations associated to three ICP-MS readings are reported.
§ is referred to a possible outlier. Whenever the case, duplicate analysis was carried out in order to exclude any instrumental problem.

Table 16 – Copper concentration in liver samples.

Liver				
	Rat #	Dry Sample (mg)	Cu (mg/Kg)	SD (mg/Kg)
1C	11	289.2	11.13	0.09
1C	12	209.1	12.06	0.01
1C	13	306	13.21	0.09
1C	14	212.3	12.12	0.11
3C	39	225.7	12.37	0.06
3C	40	200.1	13.73	0.06
3C	41	241.7	12.32	0.05
3C	42	203.7	13.85	0.04
5C	67	201.5	14.15	0.01
5C	68	217.1	13.02	0.07
5C	69	200.9	13.20	0.05
5C	70	205	13.21	0.04
7C	95	222.6	12.50	0.08
7C	96	241.3	12.13	0.05
7C	97	212.6	11.81	0.07
7C	98	255.2	10.18	0.02
9C	123	232	14.65	0.10
9C	124	209	13.82	0.04
9C	125	313	13.05	0.02
9C	126	212.6	13.63	0.10
1D	15	244.9	11.32	0.05
1D	16	244.4	11.52	0.10
1D	17	229.8	11.15	0.06
1D	18	269.3	10.76	0.05
3D	43	243.9	10.88	0.01
3D	44	221.7	11.81	0.05
3D	45	288	12.56	0.04
3D	46	225.3	11.99	0.08
5D	71	310.4	11.30	0.04
5D	72	309.6	11.03	0.04
5D	73	252.9	12.27	0.02
5D	74	239.5	11.00	0.02
7D	99	332.1	11.76	0.02
7D	100	211.1	11.54	0.07
7D	101	294	12.44	0.01
7D	102	212.5	11.78	0.08
9D	127	300	12.08	0.15
9D	128	229	10.68	0.03
9D	129	302	11.49	0.03
9D§	130	338.5	5.15	0.03

Table 17 – Copper concentration in brain samples.

Brain				
	Rat #	Dry Sample (mg)	Cu (mg/Kg)	SD (mg/Kg)
1C	11	206.8	7.92	0.02
1C	12	194.2	8.03	0.05
1C	13	187.3	7.89	0.02
1C	14	205.9	8.34	0.03
3C	39	225.8	8.45	0.04
3C	40	221.6	8.40	0.02
3C	41	206.6	8.43	0.05
3C	42	192.8	9.03	0.01
5C	67	227.2	7.62	0.02
5C	68	174.0	8.33	0.08
5C	69	220.0	8.17	0.04
5C	70	233.3	7.68	0.08
7C	95	211.3	8.22	0.02
7C	96	208.6	8.17	0.05
7C	97	213.0	7.96	0.07
7C	98	207.2	7.82	0.04
9C	123	201.1	8.14	0.05
9C	124	227.4	7.04	0.04
9C	125	210.4	8.58	0.06
9C	126	208.7	7.06	0.05
1D	15	231.1	8.07	0.01
1D	16	205.7	8.96	0.07
1D	17	193.0	8.31	0.07
1D	18	234.5	8.09	0.02
3D	43	201.6	8.24	0.12
3D	44	238.8	7.97	0.04
3D	45	195.4	8.99	0.04
3D	46	215.0	8.56	0.07
5D	71	235.9	7.30	0.03
5D§	72	205.9	20.93	0.15
5D	73	213.7	9.82	0.06
5D	74	221.1	8.56	0.10
7D	99	197.2	8.64	0.03
7D	100	197.5	7.74	0.03
7D	101	215.5	7.96	0.04
7D	102	233.7	7.38	0.06
9D	127	186.5	7.91	0.03
9D	128	226.5	8.13	0.03
9D	129	181.3	8.76	0.08
9D	130	229.7	7.92	0.01

Table 18 – Copper concentration in kidney samples.

Kidney				
	Rat #	Dry Sample (mg)	Cu (mg/Kg)	SD (mg/Kg)
1C	11	219.6	26.9	0.4
1C	12	266.4	32.0	0.4
1C	13	272.5	30.6	0.1
1C	14	219.5	35.3	0.1
3C	39	202.0	29.9	0.2
3C	40	209.4	24.7	0.2
3C	41	248.4	26.5	0.1
3C	42	205.6	35.2	0.7
5C	67	211.7	27.6	0.4
5C	68	300.0	26.9	0.3
5C	69	278.3	22.9	0.2
5C	70	229.0	35.4	0.5
7C	95	265.4	24.9	0.2
7C§	96	205.6	12.1	0.1
7C§	97	203.0	41.0	0.3
7C	98	215.6	34.1	0.1
9C	123	257.0	32.7	0.1
9C	124	232.5	25.8	0.3
9C	125	290.7	35.2	0.1
9C	126	217.5	31.7	0.2
1D	15	340.9	32.8	0.3
1D	16	294.0	31.0	0.2
1D§	17	243.9	39.7	0.2
1D	18	261.6	30.7	0.2
3D	43	255.5	25.6	0.4
3D	44	273.1	29.8	0.3
3D	45	245.5	35.2	0.3
3D§	46	286.6	40.9	0.3
5D	71	211.1	29.2	0.2
5D	72	262.5	31.3	0.2
5D	73	218.7	33.4	0.5
5D	74	235.9	26.9	0.2
7D	99	219.8	27.6	0.3
7D	100	264.4	34.1	0.4
7D§	101	280.1	47.6	0.5
7D	102	284.2	24.6	0.1
9D§	127	247.6	39.1	0.2
9D	128	320.0	25.9	0.2
9D	129	307.4	20.1	0.2
9D§	130	217.3	40.6	0.4

Table 19 – Copper concentration in lung samples.

Lung

	Rat #	Dry Sample (mg)	Cu (mg/Kg)	SD (mg/Kg)
1C	11	237.4	7.46	0.02
1C	12	259.6	7.73	0.05
1C	13	242.3	5.07	0.02
1C	14	205.7	7.14	0.04
3C	39	264.1	12.97	0.13
3C	40	211.1	15.89	0.15
3C	41	217.0	13.17	0.02
3C	42	203.0	18.37	0.17
5C	67	236.3	38.63	0.26
5C	68	311.2	35.96	0.11
5C	69	255.8	43.26	0.55
5C	70	237.0	39.94	0.47
7C	95	220.5	13.64	0.15
7C	96	307.6	13.36	0.06
7C	97	211.7	12.66	0.11
7C	98	198.3	12.21	0.03
9C	123	293.2	38.17	0.15
9C	124	275.7	39.38	0.49
9C	125	252.4	39.64	0.18
9C	126	255.2	39.79	0.18
1D	15	195.9	10.90	0.05
1D	16	264.4	7.15	0.06
1D	17	205.9	7.27	0.11
1D	18	226.5	6.79	0.07
3D	43	264.7	9.17	0.04
3D	44	326.7	6.74	0.06
3D	45	251.9	6.59	0.06
3D	46	254.3	9.00	0.01
5D	71	242.7	5.70	0.03
5D	72	275.9	6.97	0.04
5D	73	206.6	8.40	0.09
5D	74	231.5	6.01	0.04
7D	99	220.9	7.85	0.04
7D	100	218.4	8.62	0.02
7D	101	252.2	10.05	0.05
7D	102	202.6	6.04	0.04
9D	127	230.8	11.21	0.09
9D	128	280.2	6.40	0.01
9D	129	220.0	8.37	0.05
9D	130	232.5	6.51	0.05

Table 20 – Copper concentration in spleen samples.

Spleen				
	Rat #	Dry Sample (mg)	Cu (mg/Kg)	SD (mg/Kg)

1C	11	210.0	4.7	0.2
1C	12	269.0	4.6	0.3
1C	13	235.2	4.7	0.0
1C	14	214.0	4.5	0.1
3C	39	196.1	4.4	0.0
3C	40	223.7	4.6	0.2
3C	41	196.4	4.8	0.0
3C	42	228.3	4.6	0.2
5C	67	246.2	4.8	0.1
5C	68	195.5	5.3	0.1
5C	69	236.7	4.9	0.3
5C	70	212.6	5.0	0.1
7C	95	204.6	4.4	0.1
7C	96	230.4	4.8	0.1
7C	97	190.2	4.9	0.1
7C	98	221.0	4.5	0.1
9C	123	200.7	6.5	0.1
9C	124	213.2	5.2	0.1
9C	125	175.5	4.6	0.2
9C	126	253.4	4.6	0.1
1D	15	295.3	4.9	0.5
1D	16	252.6	4.5	0.1
1D	17	250.1	5.1	0.1
1D	18	252.7	5.0	0.1
3D	43	268.3	4.3	0.2
3D	44	284.5	7.5	0.1
3D	45	232.6	6.1	0.1
3D	46	255.7	4.2	0.0
5D	71	205.1	5.0	0.2
5D	72	236.6	5.0	0.3
5D	73	286.6	4.8	0.1
5D	74	204.5	5.8	0.3
7D	99	324.8	5.3	0.0
7D	100	216.5	5.0	0.3
7D	101	212.4	4.8	0.1
7D	102	203.2	4.5	0.1
9D	127	329.6	4.7	0.1
9D	128	261.0	4.7	0.2
9D	129	209.0	5.1	0.0
9D	130	220.1	6.1	0.3

Table 21 – Copper concentration in heart samples.

Heart				
	Rat #	Dry Sample (mg)	Cu (mg/Kg)	SD (mg/Kg)
1C	11	197.8	19.63	0.01

1C	12	313.2	17.27	0.11
1C	13	296.3	18.47	0.13
1C	14	231.9	18.65	0.07
3C	39	228.5	16.75	0.11
3C	40	218.6	18.15	0.01
3C	41	216.7	15.88	0.02
3C	42	237.9	18.44	0.17
5C	67	280.7	17.60	0.09
5C	68	240.5	19.95	0.07
5C	69	215.3	17.65	0.07
5C	70	252.5	19.80	0.13
7C	95	320.0	17.38	0.08
7C	96	292.1	18.43	0.08
7C	97	280.9	13.92	0.13
7C	98	232.1	21.21	0.02
9C	123	284.9	19.46	0.05
9C	124	279.6	22.09	0.10
9C	125	286.9	16.90	0.09
9C	126	258.0	17.85	0.10
1D	15	289.3	17.37	0.13
1D	16	265.2	19.49	0.15
1D	17	228.4	18.20	0.13
1D	18	226.2	17.11	0.14
3D	43	227.0	18.14	0.10
3D	44	203.0	19.06	0.13
3D	45	206.5	16.95	0.05
3D	46	240.5	16.83	0.06
5D	71	203.1	23.44	0.03
5D	72	312.7	16.59	0.03
5D	73	231.8	18.40	0.19
5D	74	190.0	16.83	0.15
7D	99	233.8	16.99	0.06
7D	100	298.9	15.59	0.03
7D	101	275.2	17.43	0.05
7D	102	214.5	15.68	0.06
9D	127	224.7	15.86	0.08
9D	128	213.4	14.36	0.08
9D	129	225.5	17.83	0.02
9D	130	254.8	17.36	0.07

STOS - pristine CuO NPs and $CuCO_3$

Organs and tissues from rats exposed to short term oral studies, with the aim to compare the toxicity of pristine CuO and $CuCO_3$, were received by UNIVE on 30/06/2016 and 25/08/2016 and listed in Table 22. The quantification of Cu in tissues and organs from

this STOS has been carried out by UNIVE.

Table 22 – List of organ and tissues, autopsy day and the nominal concentration tested from short term oral studies.

CuO	weight (g)									
sample N°	liver	lung	kidney	spleen	mln	thymus	testis	cortex	autopsy day	bodyweight (mg/kg)
5	3.7388	0.9096	0.5602	0.3455	0.0789	0.336	1.6183	0.196	5	512
6	4.1102	0.9078	0.9496	0.2803	0.084	0.2614	1.6342	0.173		
7	4.9214	0.9396	1.2983	0.3122	0.1128	0.3582	1.8305	0.158		
8	3.0603	0.8317	1.1351	0.1656	0.0525	0.1293	1.4149	0.189		
1	2.4193	0.7219	1.1848	0.1513	0.0397	0.2342	1.4311	-	6	vehicle control
2	1.8952	0.6147	0.9852	0.1441	0.045	0.2485	1.2113			
3	2.6302	0.64	1.0109	0.1503	0.0532	0.2346	1.2965			
4	2.941	0.647	1.0427	0.1349	0.0394	0.2547	1.3295			
24	2.9581	0.6882	1.1636	0.1518	0.0694	0.1903	1.3561			32
25	2.2747	0.702	0.8775	0.2203	0.0442	0.3024	1.4002			
26	1.127	0.6328	0.7665	0.1878	0.0496	0.2543	1.3594			
27	2.4246	0.71	1.0342	0.1642	0.0364	0.225	1.3318			
28	2.9367	0.798	1.1664	0.188	0.0668	0.2863	1.5035			
29	2.8192	0.7494	0.9746	0.1638	0.0215	0.239	1.4502		7	64
30	2.542	-	1.0869	0.236	0.0466	0.236	1.4033			
55	3.2386	0.6985	1.2328	0.1462	0.0726	0.2536	1.5618			32
56	2.5705	0.7316	1.3268	0.181	0.0745	0.1946	1.4945			
57	3.0414	0.8091	1.6409	0.2711	0.054	0.2846	1.4891			
58	2.7284	0.6986	1.1361	0.1854	0.0571	0.1934	1.4339			
CuCO3	weight (g)									
sample N°	liver	lung	kidney	spleen	mln	thymus	testis	cortex	**autopsy day**	**bodyweight (mg/kg)**
57	3.8663	0.8191	1.2396	0.414	0.0696	0.2624	1.7194	0.184	5	vehicle control
58	4.1446	0.9378	1.1892	0.3056	0.0516	0.3974	1.7354	0.142		
59	3.4961	0.8117	1.0445	0.2434	0.1215	0.3597	1.7217	0.15		
60	4.1484	0.8434	1.1055	0.3708	0.1263	0.3442	1.4963	0.19		
65	5.6671	1.2242	1.3505	0.3614	0.0692	0.4602	1.6581	0.118		64
66	5.1973	0.7733	1.0476	0.3146	0.0799	0.2277	1.4981	0.172		
67	6.6162	0.9271	1.1636	0.4558	0.0948	0.4772	1.9076	0.237		
68	4.1755	0.9093	0.9108	0.3423	0.1256	0.3585	1.5404	0.161		
61	2.6005	0.8916	0.6967	0.1869	0.074	0.1515	1.3435	0.192		128
62	1.934	1.0281	1.0673	0.1638	0.0762	0.074	1.5035	0.168		
63	4.2407	0.7999	1.5086	0.2245	0.0708	0.1433	1.6834	0.17		
64	3.0686	0.7572	0.9799	0.1357	0.038	0.1015	1.4675	0.147		
91	2.5654	0.6989	0.8211	0.109	0.0717	0.0904	1.3563	0.206		
92	3.6813	0.7788	0.7965	0.226	0.0884	0.1441	1.4362	0.181		
89	3.437	0.8559	1.3388	0.1651	0.0528	0.0662	1.5889	0.13	6	
90	3.4539	0.8629	1.2989	0.2429	0.0919	0.0911	1.7374	0.205		
85	6.902	1.06	1.201	0.497	0.088	0.278	1.664	0.171	26	vehicle control
86	4.871	1.045	1.285	0.373	0.078	0.498	1.708	0.191		
87	7.426	1.068	1.526	0.356	0.086	0.481	1.828	0.167		
88	6.232	0.964	1.489	0.275	0.083	0.298	1.75	0.183		
93	6.846	1.131	1.489	0.358	0.0345	0.303	1.702	0.174		64
94	6.391	1.043	1.375	0.28	0.054	0.368	1.767	0.131		
95	5.464	0.812	1.061	0.39	0.07	0.346	1.559	0.09		
96	5.841	0.843	1.341	0.422	0.083	0.459	1.851	0.025		

Materials and methods

Acid digestion

The acid mixture used for samples mineralization included HNO_3 (trace select ultra 69%, Sigma-Aldrich <0.5µg/Kg), H_2O_2 (trace select ultra 30%, Sigma-Aldrich <0.05µg/Kg), in a 2:1 ratio. The microwave system ETHOS 1600, Milestone was used to digest the samples,

following the procedure reported in Table 5Table 15. Afterwards, the samples were allowed to cool down for 30 minutes at room temperature. The obtained solutions were transferred in PTFE tubes and diluted to 25 mL with MilliQ water.

ICP-MS analysis

An aliquot of each sample solution was properly diluted and analyzed by inductively coupled plasma mass spectrometry equipped with single channel Universal Cell (sp-ICP-MS NexION 350XXD, Perkin Elmer).
Isotope ^{65}Cu was selected to quantify Cu because of the less polyatomic interferences (e.g. $^{40}Ar^{23}Na$) than isotope ^{63}Cu. Moreover, to decrease interferences Kinetic energy discrimination (KED) was employed, using He as collision gas. Samples were quantified by external calibration method using a multi-point curve (blank and 10 points over the concentration range from 0.5 µg L^{-1} to 5000 µg L^{-1}). Yttrium at 5 µg·L^{-1} was used as internal standard.

QA/QC

Potential contamination from the laboratory was controlled by adding at least one reagent blank during each digestion session.
The limit of detection (LOD) and the limit of quantification (LOQ) were calculated for each sample set as the average of blanks + 3 standard deviation (SD) and as the average of blanks + 10 SD, respectively.
In order to verify the accuracy and repeatability of the method, 6 aliquots of the standard reference material (SRM) NIST 1577c (bovine liver) were analysed every 10 samples.

Results

Accuracy

The average Cu concentration detected in the SRM was 277 ± 5 mg·kg^{-1}, in satisfactory agreement with the reference value (262 ± 2 mg·kg^{-1}).

Recovery

With respect to the certified value, the recovery of Cu ranged from 90 to 100%.

BEC

BEC is the background concentration signal providing the actual magnitude of noise. The detected BEC value was 0.16 µg·L^{-1}.

LOD/LOQ

Average blank values, LOD and LOQ were calculated by considering both the reagent and the control blanks. Detected LOD and LOQ value were, respectively, 20 ng·L^{-1} and 68 ng·L^{-1}.

Copper concentration in analysed organs

Copper concentration in tissues and organs from rats exposed to STOS, expressed on a dry weight basis, are shown in Tables 23 and 24. Average values and relative standard deviations % associated to three ICP-MS readings are reported.
In yellow possible outliers are highlighted. Whenever the case, duplicate analysis was carried out in order to exclude any instrumental problem.

was shown for all the samples both in AFW and AMW, except for CuO-PEI which showed an higher stability in AFW, resulting in agreement with hydrodynamic size and ζ-pot values (see Table 1 and 2).

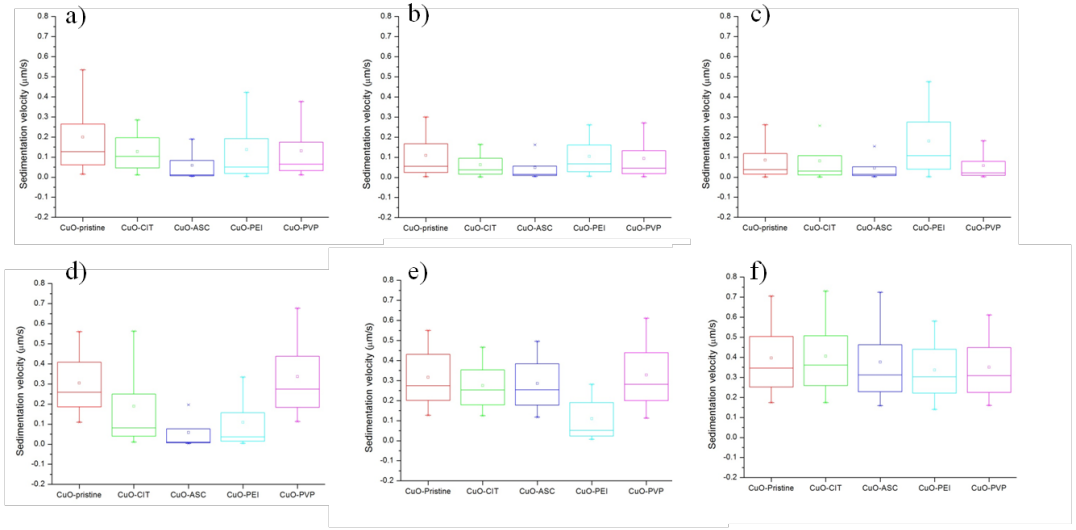

Figure 4 – Sedimentation velocity distribution of pristine and modified CuO NPs dispersed in a) MQ, b) MEM, c) DMEM, d) PBS e) AFW and f) AMW.

Ions release data, determined by the ionic copper dissolved to total copper ratio through ultra-centrifugation followed by ICP-OES analysis, are presented in Table 3. Generally, it can be stated that the dissolution process occurred within the first hour. Moreover, data collected in MEM and DMEM showed that the dissolution greatly increased in both biological media compared to values in MilliQ, PBS, AFW and AMW media.

Table 3. $Cu_{dissolved}/Cu_{total}$ weight ratio % of pristine and modified CuO samples dispersed in different media after 24 h at 25 °C (in MilliQ and environmental media) and at 37 °C (in biological media).

	$Cu_{dissolved}/Cu_{total}$ weight ratio %

CuO-ASC	2.1 (0.6)	2 (0.5)	<0.3 (0.1)	34 (0.5)	48 (0.3)	50 (0.6)	65 (0.4)	1.2 (0.8)	0.7 (0.7)	4.5 (1)	0.7 (1.1)
CuO-PEI	1.7 (0.7)	2.8 (0.6)	2.5 (0.6)	28 (0.3)	43 (0.3)	49 (1)	66 (1.3)	6.9 (1)	6.3 (0.9)	3.2 (1.1)	7.4 (0.5)
CuO-PVP	0.8 (0.3)	0.2 (1)	<0.3 (0.1)	40 (0.4)	34 (0.4)	57 (0.7)	67 (0.5)	0.02 (0.1)	0.1 (2.8)	0.1 (0.3)	0.1 (1.6)

Taking into account the dissolution experiments for all the dispersions performed in DMEM, $Cu_{dissolved}/Cu_{total}$ ratio reached values between 65 and 69% after 24h. As far as dissolution experiments in MEM, dissolution rate was slightly lower compared with data recorded in DMEM, ranging from 34 to 59% after 24h. One of the reason of the high dissolution rate of CuO NPs in the biological media tested can be ascribed to the chelating effect of amino acids and proteins (Midander et al., 2009; Semisch et al., 2014; Mudunkotuwa and Grassian 2015). Taking into account the different composition of the media tested, the general low CuO NPs solubility rate observed in both MilliQ and PBS (dissolution< 3%), as well as in AFW and AMW (dissolution < 8%) further confirmed the primary role of protein components that promote dissolution. Among all the media, CuO NPs dissolution rate reached the highest values in DMEM because contains approximately four times as much of glucose, amino acids and vitamins with respect to MEM.